Abstract

Studies on the regulation of PKA-mediated lipolysis

Jung Hyun Lee

School of Biological Sciences

The Graduate School

Seoul National University

Lipolysis is a delicate process regulated by complex signaling cascades and sequential enzymatic activations. Among them, PKA signaling is known to be one of key pathways that influence lipolysis. Genetic studies on the roles of PKA in lipolysis with mouse models appear to have various limitations including complexity of PKA subunits and in vivo compensatory effects. In this study, I have used *Caenorhabditis elegans* and mammalian adipocytes as model systems to investigate PKA function and genes involved in PKA-mediated lipolysis. *C. elegans* and mammalian adipocytes are complementary systems to test PKA because PKA activity can be effectively modulated by knockdown or chemicals.

In *C. elegans*, fasting induces various physiological changes, including a dramatic decrease in lipid contents through lipolysis. Interestingly, *C. elegans* lacks perilipin family genes which play a crucial role in the regulation of lipid homeostasis in other species. Here, I

demonstrate that in intestinal cells of *C. elegans*, fasting increases cAMP levels, which activates PKA to stimulate lipolysis via Adipose TriGlyceride Lipase-1 (C05D11.7; ATGL-1) and a newly identified gene LIpid Droplet protein-1 (C25A1.12; LID-1). LID-1 modulates lipolysis by binding and recruiting ATGL-1 during nutritional deprivation. In fasted worms, lipid droplets were decreased in intestinal cells, whereas suppression of ATGL-1 via RNAi resulted in retention of stored lipid droplets. Overexpression of ATGL-1 markedly decreased lipid droplets, whereas depletion of LID-1 via RNAi prevented the effect of overexpressed ATGL-1 on lipolysis. Moreover, ATGL-1 protein stability and LID-1 binding was augmented by PKA activation, eventually leading to increased lipolysis. In addition, through the ethylmethane sulfonate (EMS) mutagenesis screening in *C. elegans*, I have isolated three mutants that suppress PKA function. These mutant suppressed dumpy morphology and restored Nile Red-stained granules induced by *kin-2* RNAi. Since the identification of suppressor genes has not been completed, further studies are required for the identification of the gene(s) of interest.

In the study using mammalian adipocytes, combinatorial siRNA transfection have revealed that, among four regulatory subunits of PKA, RIα and RIIβ subunits are required for the inhibition of lipolysis and lipid droplet maintenance under basal state. Knockdown of RIα and RIIβ subunits increased glycerol release and decreased lipid droplets without any lipolytic stimulus. Interestingly, knockdown of regulatory subunits increased ATGL protein level, which would play a key role in PKA-mediated lipolysis. Furthermore, I observed that the expression of PKA RIIβ subunit was decreased in high-fat diet (HFD) fed mice, indicating potential roles of PKA subunits in lipolysis and hyperlipidemia. Taken together, these data suggest the crucial role of PKA activity in lipid homeostasis with concerted action of lipase and lipid droplet protein.

Keywords : Protein kinase A, lipolysis, ATGL, lipid droplet

Student number : 2007 - 20359

Table of Contents

Abstract……...……i

Table of Contents…….……iv

List of Figures……...vi

List of Tables……ix

I. Introduction

I-1. Energy homeostasis and lipid metabolism……...……...……1

I-2. Lipases and regulation of lipolysis in adipocytes……..….2

I-3. Protein kinase A ……...…..3

I-4. *C. elegans* as a model organism for studying lipid metabolism……..…5

I-5. The purpose of this study……...…….7

II. Materials and Methods……..8

III. Results

III-1. LID-1/ATGL-1 mediated lipolysis upon fasting in *C. elegans*……..……16

III-2. Genetic screening for the mediator of PKA-induced lipolysis in *C. elegans*……42

IV-3. PKA subunit balance and lipolysis in mammalian adipocytes……...55

IV. Discussion……..70

V. Conclusion and perspectives……..78

VI. References…….80

Abstract in Korean……...……90

List of Figures

Figure 1. Fasting decreases Oil Red O staining in the anterior intestine……17

Figure 2. ATGL-1 is a major lipase for fasting-induced lipolysis in *C. elegans*……..18

Figure 3. ATGL-1 protein level is increased upon fasting in *C. elegans*……..19

Figure 4 ATGL and CGI-58, not perilipin, are conserved in *C. elegans*…….....21

Figure 5. *lid-1*, C25A1.12, is a homolog of CGI-58 and localizes to lipid droplets……22

Figure 6. *lid-1* mRNA expression and localization of LID-1::GFP does not change during fasting……..24

Figure 7. LID-1 is a lipid droplet protein required for fasting-induced lipolysis……25

Figure 8. C37H5.2 and C37H5.3 are not required for fasting-induced lipolysis……26

Figure 9. LID-1 is required for ATGL-1 activity……..27

Figure 10. PKA signaling mediates fat mobilization upon fasting in *C. elegans*……29

Figure 11. AMPK signaling is not required for fasting-induced lipolysis……30

Figure 12. *atgl-1* and *lid-1* act in downstream of PKA signaling……31

Figure 13. PKA phosphorylates ATGL-1……33

Figure 14. PKA activation increases ATGL-1 protein level……34

Figure 15. PKA regulates ATGL-1 protein stability as well as LID-1 binding……36

Figure 16. *atgl-1* and *lid-1* are required for energy production during fasting……37

Figure 17. RNAi of *atgl-1* or *lid-1* does not alter genome-wide gene expression upon fasting.....40

Figure 18. Working model of fasting-induced lipolysis in *C. elegans*…… 41

Figure 19. RNAi of *kin-1* and *kin-2* affects basal PKA activity……...43

Figure 20. RNAi of *kin-1* and *kin-2* alters morphology and distributions of lipid staining dyes. ……..44

Figure 21. PKA activation depletes intestinal lipid storage……46

Figure 22. Scheme of *kin-2* RNAi suppressor mutagenesis screening……47

Figure 23. Isolated mutants rescues *kin-2* RNAi phenotypes……48

Figure 24. Whole-genome sequencing and candidate genes……53

Figure 25. Expressions of PKA subunits are tissue-specific……56

Figure 26. Ca and RIIβ subunits of PKA expressions are increased during adipogenesis….....57

Figure 27. PKA subunit stoichiometry model……..58

Figure 28. Knockdown efficiencies of siRNAs targeting PKA subunits are confirmed……..59

Figure 29. Knockdown of all regulatory subunits of PKA result in increased basal lipolysis in 3T3-L1 adipocytes……60

Figure 30. RIα and RIIβ subunits are necessary and sufficient factors for maintaining basal lipolysis……62

Figure 31. Knockdown of PKA regulatory subunits depletes lipid droplets in adipocytes……..63

Figure 32. Knockdown of PKA regulatory subunit changes lipid metabolism gene expressions……64

Figure 33. Effects of PKA regulatory subunit knockdown is partially suppressed by knockdown of ATGL……66

Figure 34. PKA activation increases ATGL expression in 3T3-L1 adipocytes……67

Figure 35. Expression of PKA RIIβ subunit is down-regulated in adipose tissue of HFD-fed mice……..69

List of Tables

Table 1. Gene set enrichment analysis of fasting-responsive genes…….39

Table 2. Chromosome mapping result of mutant #1……50

Table 3. Chromosome mapping result of mutant #2……..51

Table 4. Chromosome mapping result of mutant #3……52

Table 5. List of candidate genes obtained from *kin-2* RNAi suppressor screening……..54

I. Introduction

I-1. Energy homeostasis and lipid metabolism

Biological processes require for energy in living system. In aspect of bioenergetics homeostasis, maintaining balance between energy intake and energy expenditure is the most critical issue for organisms. In animals, energy can only be produced by metabolizing nutrient molecules. When food is plenty, animals take in energy from feeding. However, when food is scarce, animals must utilize nutrients stored in the internal tissues to meet the energy requirement of the body. Thus, animals should modulate metabolic pathways upon changes in food availability.

Fasting is the most prevalent environmental condition that alters energy metabolism of an animal. To endure fasting, animals have evolved energy storing tissues. Energy storage and utilization processes appear to be critical for maintenance of energy homeostasis in fluctuating environments. Triglyceride is a neutral lipid molecule, which is composed of glycerol and 3 fatty acids, and is widely used for energy storage across animal kingdom. There are several advantages of storing energy in the form of triglyceride. Triglyceride is an energy rich molecule, and it can be stored compactly relative to its volume because it is hydrophobic and does not require hydration. Lastly, triglyceride molecule has non-colligative property so it can be stored in large amount without altering osmotic pressure.

Most neutral lipids, including triglyceride and cholesterol esters, are stored in the form of lipid droplets in cytoplasm. Lipid droplet is a highly dynamic organelle involved in cellular lipid homeostasis [1] and numerous proteins have been shown to associate with lipid droplets [2, 3]. The perilipin family is one of the most well-studied lipid droplet proteins conserved from

Dictyostelium to mammals [4, 5]. These perilipin family of lipid droplet proteins play crucial roles in lipid homeostasis [5-7]. It has been shown that perilipin 1 (Plin1) serves as a barrier to lipases as inferred by elevated basal lipolysis in Plin1 null mice. In addition, Plin1 is required for maximal lipolytic activity via recruitment of lipase protein upon lipolytic signals [8, 9].

In mammals, adipocytes, as energy reservoirs, sense and integrate various endocrine signals to modulate lipolytic activity. Fatty acids released from adipocytes are subsequently transported to other target tissues and are used as key substrates for energy production via fatty acid oxidation [10]. On the other hand, excess accumulation of intracellular lipids in ectopic fat tissues often impairs physiological responses due to lipotoxicity [11]. Thus, it is crucial to decipher how lipases are temporally and spatially regulated to access lipid droplets in response to nutritional changes.

I-2. Lipases and regulation of lipolysis in adipocytes

In mammalian adipocytes, hormone-sensitive lipase (HSL) was the first enzyme discovered to hydrolyze lipids. HSL is a neutral lipase and hydrolyzes triglyceride, diacylglycerol, and cholesteryl esters. However, in vitro assays showed that HSL has greater hydrolase activity to diacylglycerol than triglyceride [12]. HSL activity is regulated by phosphorylation and translocation. Upon hormonal stimulation, HSL is phosphorylated by protein kinase A (PKA) at multiple sites and translocates from cytosol to lipid droplet [13-15]. Translocation of HSL requires for lipid droplet protein perilipin 1, which is also phosphorylated upon PKA activation [8, 16], and the activity of HSL is enhanced by the presence of FABP4 [17]. Phenotypes of HSL null mice include complete loss of cholesterol ester hydrolase activities, accumulation of diacyglycerol in adipose tissues, adipocyte hypertrophy, and male sterility [18-20]. Unexpectedly, HSL deficiency does not cause obesity and substantial fraction

of triglyceride hydrolase activity is retained.

ATGL is an important enzyme that mediates hydrolysis of intracellular triglyceride [21-23]. In contrast to HSL-deficient mice, ATGL-knockout mice show severe lipid accumulation in many organs including adipose tissue and heart, indicating that ATGL is the rate-limiting enzyme in triglyceride hydrolysis [24]. ATGL mRNA expression is markedly increased by fasting [21] and reduced by insulin signaling [25-27]. ATGL activity is greatly enhanced by binding to comparative gene identification-58 (CGI-58; ABHD5) [28]. In basal state, CGI-58 is associated with perilipin 1, whereas PKA activation leads to dissociation of CGI-58 from perilipin 1 and promotes its binding with ATGL [29-32].

Many studies over last 40 years have revealed that cAMP-PKA axis forms a critical node in the regulation of lipolysis in adipocytes. Major components of lipolytic pathways are direct targets of PKA and, recently, ATGL also has been reported to be a target of PKA [33]. Furthermore, most extracellular signals that control lipolysis act through the cAMP-PKA axis. Catecholamine binds to beta adrenergic receptors and activates adenylyl cyclase, producing cyclic AMP (cAMP), which acts as an activator of protein kinase A (PKA). Insulin, conversely, can activate phosphodiesterase 3B and reduces cAMP levels [34-36]. Receptors for other anti-lipolytic signals such as adenosine [37] and nicotinic acid [38] are coupled with inhibitory G proteins that suppress adenylyl cyclase. Besides, tumor necrosis factor-alpha (TNFα) has been known to be a long-term regulatory factor of lipolysis while not directly linked with PKA signaling. TNFα down-regulates perilipin expression and promotes lipolysis [39, 40], and it is considered as one of the factors for elevated lipolysis in obesity. Taken together, it is likely that PKA is the most important signaling mediator of lipolysis upon physiological and hormonal changes.

I-3. Protein kinase A

A number of extracellular signaling molecules use cyclic adenosine 3'5'-monophosphate (cyclic AMP; cAMP) as an intracellular second messenger. Protein kinase A (PKA) is a cyclic AMP-dependent serine/threonine kinase that mediates a majority of cAMP signal transduction. Since it has been discovered in 1950s [41-44], cyclic AMP-PKA system became one of the best understood signaling pathways in terms of biochemical properties. In the absence of cAMP, PKA is an inactive tetramer composed of four subunits - two regulatory subunits and two catalytic subunits. In the presence of cAMP, the regulatory subunit of PKA binds to cAMP and its affinity for the catalytic subunit decreases by approximately 10^4-fold, releasing active catalytic subunits to phosphorylate target proteins [45, 46]. Structural analyses have revealed that regulatory subunits of PKA undergo substantial conformational changes dependent on cAMP binding, which is essential for the inhibition and activation of catalytic subunits [47, 48].

There are four regulatory subunit genes, RIα, RIβ, RIIα, and RIIβ, and two catalytic subunit genes in rodents (three in humans), Cα and Cβ [49]. The primary function of the regulatory subunit is to inhibit and regulate catalytic subunit activity. Regulatory subunits of PKA have been categorized into two groups, type I and type II, on the basis of the holoenzyme elute from anion exchange resins [50]. These subunits have been shown to have different tissue distributions and have different biochemical properties. It has been reported that RI subunits have higher affinity for cAMP than RII subunits [51-54], whereas their affinities for catalytic subunits are similar [55].

PKA has a wide range of substrates and is involved in a number of physiological processes. Hundreds of PKA target proteins have been identified and, still, new substrates for PKA are continually being reported [56, 57]. For a better appreciation of the role of PKA in vivo,

mouse models with genetic manipulation of PKA subunit have been studied. However, deletion of some PKA subunits caused severe phenotypes, such as embryonic lethality in case of RIα [58, 59] and growth defect, high frequency of perinatal death, and male sterility in case of Cα [60]. Knockout mice of Cβ [61] or RIβ [62] show more subtle and tissue-specific phenotypes, such as defects in learning and memory. Mice lacking RIIα are healthy and have no clear phenotypes [63]. RIIβ knockout mice are morphologically normal and fertile, despite reduced adiposity [64]. In addition, mice lacking RIIβ are protected from diet induced obesity and insulin resistance [65]. It has been suggested that loss of RIIβ gene results in up-regulation of RIα subunit, which leads to increased cAMP sensitivity and higher basal lipolysis in adipocyte [66, 67]. Thus, studies using genetic mouse models have revealed the importance of PKA signaling pathways. However, due to the severity of phenotype or the compensatory effect of other subunits, it appears that mouse models would have limitations in understanding the role of PKA subunits.

I-4. *C. elegans* as a model organism for studying lipid metabolism

Caenorhabditis elegans has received much attention as a genetically tractable model organism for studying the molecular mechanisms of adaptive responses to nutritional changes [68, 69]. *C. elegans* has its own developmental programs for nutritional adaptations. For instance, at multiple stages of larval development, food deprivation halts the developmental process and promotes entry into the diapause state [70]. In addition, during larval stage 2 (L2), *C. elegans* can enter an alternative developmental stage, called dauer, to withstand long periods of starvation [71, 72]. In adult worms, food availability influences diverse aspects of physiological responses, including metabolic gene expression [73], locomotive behavior [74], pharyngeal pumping [75], germ line stem cell proliferation [76], and egg laying [77, 78].

Like mammals, *C. elegans* store large amounts of lipids in intestinal cells and hypodermis. C. *elegans* expresses most key metabolic genes conserved in mammals, such as PKA, SREBP, AMPK, C/EBP, TOR, and nuclear hormone receptors [79-83]. Based on sequence homology, *C. elegans* has at least 32 genes which are annotated as potential lipases, and a subset of lipases has been reported to function in long-term survival of dauers [84], longevity [85], induction of autophagy [86], and lysosomal lipolysis during fasting [87]. Interestingly, *C. elegans* genome does not encode genes homologous to perilipin family. However, it has been reported that *C. elegans* utilizes stored lipids upon fasting [79], indicating that *C. elegans* would have own regulatory mechanisms to coordinate systemic energy homeostasis upon nutritional changes such as fasting and feeding.

In some aspects, lipid metabolisms in *C. elegans* are more complex than mammals. *C. elegans* possesses delta-3, 5, 6, 9, 12 desaturases activity and synthesize a wide variety of fatty acids [88, 89]. Genetic studies have shown that production of unsaturated fatty acids is required for normal development, survival, and fat storage of *C. elegans* [88, 90, 91]. In addition, it has been suggested that *C. elegans* uses monomethyl branched-chain fatty acids, C25ISO and C17ISO, as signaling factors for post-embryonic growth and larval development [92, 93]. Given that *C. elegans* seems to actively use lipid metabolites as signaling molecules as well as an energy source, more studies are required for better understanding of lipid metabolism in *C. elegans*.

Intestinal lipid droplets in *C. elegans* are heterogeneous. Studies using lipid-staining dyes have suggested that *C. elegans* stores lipids in its lysosome-related organelles (LRO), which are birefringent gut granules [94-96]. Previously, it has been reported that endoplasmic reticulum (ER) resident proteins IRE-1 and HSP-4 are associated with induction of fil-1 and fil-2, which are required for decrease of Nile Red-positive lipid granules upon fasting [97].

Recently, it has been suggested that in *C. elegans*, the major fat-storing organelles are distinct from LROs which are stained by the Nile Red dye in live worms [98, 99]. However, other studies have reported that Nile Red staining after fixation or Oil Red O staining correlates with biochemical triglyceride content [98, 100]. Thus, the nature of lipid droplets and how worms utilize lipid metabolites are largely unknown.

I-5. The purpose of this study

Lipolysis is regulated by a variety of factors in response to nutritional changes. Among them, PKA activity has been shown to have strong correlation with lipolytic activity. In this study, I have aimed to find out the genetic and molecular understanding of PKA-mediated lipolysis. In the first part of this study, I searched for potential downstream effectors of PKA signaling. As a result, I have identified key genes involved in fasting-induced lipolysis and their regulatory pathways in *C. elegans*. I have discovered that a newly identified lipid droplet protein LIpid Droplet protein-1 (C25A1.12; LID-1) and Adipose TriGlyceride Lipase-1 (C05D11.7; ATGL-1) coordinately mediate lipolysis to dissipate stored energy sources through PKA activation during nutritional deprivation in *C. elegans*. In the second part, I have performed random mutagenesis screening to find novel gene(s) that mediates PKA function in *C. elegans*. Through this screening, three mutants that rescue the RNAi phenotype of *kin-2*, regulatory subunit of PKA, have been identified. And identification of mutated gene is required to find a mediator of PKA-induced lipolysis. In the third part, I tried to define functional specificity of PKA subunits and their roles in lipolysis in mammalian adipocytes. Using siRNA mediated knockdown, I found that certain subunits of PKA are necessary and sufficient for regulation of lipolysis in mammalian adipocytes. In addition, I suggest that the balance between the amounts of catalytic and regulatory subunits of PKA could alter basal lipolytic activity via

increase in ATGL protein level. I also discuss the potential role of PKA subunit imbalance in adipose tissue of obesity.

II. Materials and Methods

Worm strains and culture

N2 Bristol was used as the wild-type strain. The following alleles and transgenes were used: *kin-2(ce179)*; *hjIs67*[*atgl-1p*::*atgl-1*::*gfp*]; and *Ex*[*act-5p*::*lid-1*::*gfp*]. All animals were raised at 20°C in standard nematode growth medium (NGM).

Feeding RNAi

RNAi clones were obtained from the Ahringer and Vidal RNAi library. The *kin-1* RNAi clone was generated by cloning the cDNA fragment of *kin-1*. Synchronized worms were cultured on RNAi plates until they reached the young adult stage. The efficiency of RNAi was confirmed by real-time Q-PCR using appropriate PCR primers.

Fasting assays

Synchronized L1 larvae were grown to the one-day young adult stage. Feeding group worms were harvested and washed with M9 buffer before proceeding to the next step. Except for the treatment of chemicals, worms were fasted in empty plates for 4 or 8-h, harvested, and washed. Then, the prepared worms were resuspended with buffers appropriate for further analysis. For MG132 or forskolin treatment, worms were pre-incubated in M9 buffer with *Escherichia coli* and 100 μM MG132 or 100 μM forskolin for 2-h. Then, worms were washed and incubated for additional 4-h in M9 buffer with 100 μM MG132 or 100 μM forskolin in the presence or absence of *Escherichia coli* depending feeding or fasting, respectively.

Lipid staining and quantification

Oil Red O staining was performed as previously reported [101]. Briefly, worms were harvested and resuspended in 60 μL of 1X PBS pH 7.4, 120 μL of 2X MRWB buffer, and 60 μL of 4% paraformaldehyde. The worms were frozen-thawed 3 times and washed with PBS. The worms were then dehydrated in 60% isopropyl alcohol for 10 min at room temperature and stained with Oil Red O solution. All Oil Red O images from the same experiment were acquired under identical settings and exposure times for direct and fair comparisons. Relative Oil Red O intensities were quantified using Image J software (NIH). 10 to 15 worms from each group were randomly selected for quantification. Each image was split into RGB channels and the green channel was subtracted from the red channel to eliminate non-red background signals. Anterior intestinal cell areas were selected to measure Oil Red O intensities. Fixed and Live Nile Red staining was performed as described previously [100] [68].

Biochemical triglyceride measurement

Triglyceride contents were measured using a triglyceride assay kit (Thermo scientific; Cat. TR22321). Synchronized young adult worms were resuspended in 5% Triton X-100 solution and homogenized using glass beads and Precellys 24 homogenizer (Bertin Technologies). For complete lysis and triglyceride extraction, the homogenates were sonicated and subjected to two cycles of heating (80°C) and cooling (room temperature). Then, worm extracts obtained by centrifugation were used to measure total triglyceride amount according to the manufacturer's protocol.

cAMP measurement

cAMP concentrations were measured using a direct cAMP ELISA kit (Enzo Lifescience; Cat. 25-0114), according to the manufacturer's protocol. Harvested worms were resuspended in 0.1 M HCl to inactivate phosphodiesterase. Worms were homogenized using glass beads and Precellys 24 homogenizer, after which the homogenates were sonicated. Then, worm extracts were collected by centrifugation and used for ELISA. Results were analyzed using 4 parametric logistic curve fitting models.

In vitro kinase assay

To perform an in vitro kinase assay, GST-tagged recombinant ATGL-1 (wild type, WT), ATGL-1 (S303A), and LID-1 proteins were produced from *E. coli* and purified by GST pull down. And 1 μg of each GST-protein was mixed with the PKA catalytic subunit (New England Biolabs), 10X kinase buffer (500 mM Tris-HCl [pH 7.5], 1 mM EGTA, 100 mM magnesium acetate), ^{32}P-labeled 1 mM ATP, and distilled water and incubated for 30 min at 37°C. The kinase reaction was analyzed by autoradiography after SDS-PAGE and Coomassie staining.

PKA activity assay

Synchronized young adult worms were harvested and homogenized in protein extraction buffer (20 mM Tris-HCl, 10 mM DTT, 1 mM NaF, 1 mM Na_3VO_4, 10 mM EDTA, 10 mM EGTA, and protease inhibitor cocktail). Worm extracts were sonicated and centrifuged to obtain soluble proteins. PKA activity was measured according to a previously reported protocol [102]. Briefly, 30 μg of proteins were pre-incubated with 10X kinase assay buffer (500 mM Tris-HCl, 1 mM EGTA, 100 mM magnesium acetate), 30 μM Kemptide (PKA substrate peptide) and with 25

μM dibutyryl-cAMP or 15 μM PKI at 30°C for 30 min. Then 1 mM [γ-^{32}P] ATP was added to the reaction mixture and incubated at 30°C for 10 min. The reaction was terminated by spotting the reaction mixture onto P81 phosphocellulose paper. The papers were immediately immersed in 75 mM phosphoric acid. After washing 3 times with fresh phosphoric acid, the papers were briefly rinsed with acetone and air dried. Radioactivity was measured by Cerenkov counting.

Oxygen consumption rate measurement

To measure the oxygen consumption rate, synchronized worms were cultured in RNAi plates to the one-day young adult stage. Half the worms were harvested and cultured on empty NGM plates for 4 h to prepare fasted samples. Worms were harvested just prior to measurement and were cultured in oxygen-saturated M9 buffer. The oxygen consumption rate was monitored using a Clark-type electrode sensor, YSI 5300A Oxygen Monitor (YSI Corporation). Protein content was determined using the BCA method and was used to normalize the oxygen consumption rate, which is reported as relative mmol O_2/h/mg protein.

Microarray analysis

Synchronized young adult worms were divided into well-fed and 8-h fasted samples using the fasting assay protocol described above. Total RNA was extracted using TRIzol reagent (Invitrogen) and purified using RNeasy mini kit (QIAGEN). Affymetrix *C. elegans* genome array chip was used for all microarray experiments. DAVID analysis was used to show enrichment of specific functional categories in fasting-responsive genes [103]. Pvclust was used for clustering analysis of microarray data [104].

EMS Mutagenesis screening

For the treatment of ethyl methanesulfonate (EMS), L4 stage worms were incubated in 50 mM EMS in M9 buffer for 4 hours. Worms are then harvested and washed for 5 times with M9 buffer. Mutagenized P0 worms are plated to get F1 worms. When most F1 worms are become gravid adult, F1 worms were bleached to obtain synchronized F2 eggs. Then, F2 eggs are grown on *kin-2* RNAi plates with Nile Red and used for screening. For the screening, Nile Red signal was observed using Lumar microscope (Zeiss).

Immunoprecipitation and western blotting

Cells were lysed on ice with radioimmunoprecipitation assay (RIPA) buffer (50 mM Tris-HCl [pH 7.4], 150 mM NaCl, 1 mM EDTA, 1 mM PMSF, 1% (v/v) NP-40, 0.25% (w/v) Na-deoxycholate, and protease inhibitor cocktail) and subjected to immunoprecipitation or western blotting. For immunoprecipitation, lysates were incubated with anti-Myc (Cell Signaling) or anti-Flag antibody (Sigma-Aldrich) for 12 h at 4°C. Immune-complexes were collected using protein A-sepharose beads (GE Healthcare) for 2 h at 4°C. The beads were washed 3 times with 500 μL RIPA buffer. Proteins were eluted by boiling in SDS sample buffer for 5 min, separated on SDS-PAGE, and analyzed by western blotting. For western blotting, proteins separated on SDS-PAGE were transferred to polyvinylidenedifluoride (PVDF) membranes (Millipore). The membranes were blocked with 5% (w/v) skim milk in Tris-buffered saline containing 0.1% (v/v) Tween-20 (TBST; 25 mM Tris-HCl [pH 8.0], 137 mM NaCl, 2.7 mM KCl, and 0.1% Tween-20) at room temperature for 30 min, followed by overnight incubation with primary antibodies at 4°C. Antibodies against Flag-tag (Sigma-Aldrich), Myc-tag (Cell Signaling), mouse ATGL (Cell Signaling), and GAPDH (AbFrontier) were used. The membranes were washed 3 times with TBST and hybridized with secondary antibodies conjugated with horseradish peroxidase

(Sigma-Aldrich) in 5% skim milk dissolved in TBST at room temperature for 2-h. The membranes were then washed 3 times with TBST, incubated with enhanced chemiluminescence reagents, and quantified with LuminoImager (LAS-3000) and Science Lab Image Gauge software (Fuji Photo Film). The band intensities of the lanes were quantified using Image J (NIH).

Cell culture and transfection

For transfection, HEK293T and Cos-1 cells were grown to 70% confluence and each expression vector was transfected using the calcium phosphate and lipofectamine 2000 (Invitrogen), respectively. At 6 h post-transfection, the medium was replaced with DMEM supplemented with 10% FBS and 1% AA/PS. At 24 h post-transfection, forskolin (FSK; Calbiochem) or an equal amount of dimethyl sulfoxide (DMSO; Amresco) in serum-free DMEM media was added to the corresponding plates. After incubation for 3-h, cells were harvested. For 3T3-L1 transfection, fully differentiated cells were extensively washed with PBS and treat with trypsin/EDTA. Then, cells were collected in conical tube, centrifuged for 2 min at 1,000 rpm. After washing with PBS, cells were mixed with siRNA and transfected using Microporator MP-100 (DigitalBio). Transfection condition was 1100V, 30 ms, and single pulse.

Glycerol release assay

Glycerol concentration in the medium of 3T3-L1 was measured using Free Glycerol Reagent (Sigma F6428) according to the manufacturer's protocol. Briefly, Cells were incubated with 2% fatty acid free-BSA serum free high glucose DMEM media with DMSO, forskolin (Calbiochem) or isoproterenol (Sigma). After 3 hours, medium was collected and used for assay. Total protein

amount was used for normalization.

Quantitative RT-PCR

Total RNA was isolated using TRIzol Reagent (Invitrogen, CA) according to the manufacturer's protocol. Complementary DNA was synthesized using M-MuLV reverse transcriptase with random hexamer primers (Fermentas). Quantitative RT-PCR (qRT-PCR) was performed on a CFX96 real-time system (Bio-Rad) with SYBR Green (Invitrogen). Relative expression levels of all mRNAs were normalized to *actin-1/3* mRNA.

Animal experiments

All animal experiments using mice were approved by the Seoul National University Animal Experiment Ethics Committee. For gene expression analysis, 8-week old C57BL/6 mice were used. Diet-induced obesity was induced by feeding 70% high-fat diet for 17 weeks.

Microscopy

GFP and Nile Red images were observed using Axio Observer Z1 and a confocal LSM 700 system (Zeiss). Oil Red O staining was visualized using an Axioplan II microscope and images were captured using an Axiocam HRc camera (Zeiss). Phase contrast images of cell culture was obtained using EVOS cell imaging systems (Life Technologies).

Statistical analysis

Values are shown as mean + SD. Unless otherwise mentioned, comparison of mean values was evaluated by two-way ANOVA with Bonferroni posttest. A p value less than 0.05 was considered significant.

III. Results

III-1. LID-1/ATGL-1 mediated lipolysis upon fasting in *C. elegans*

C. elegans atgl-1 is necessary for fasting-induced lipolysis

In *C. elegans*, fasting significantly decreased stored lipid droplets in anterior intestinal cells, which is consistent with previous reports (Fig. 1) [79, 98]. To identify the key lipase(s) involved in this process, I carried out reverse genetic approaches. The *C. elegans* genome has over 32 putative lipase genes. I selected 21 genes with available RNAi clones that target 9 class II lipase genes (*lips*, *fil-1*), 3 patatin domain-containing genes (*atgl-1*, D1054.1, B0524.2), 1 HSL homolog (*hosl-1*), 2 phospholipases A2 homolog (C07E3.9, C03H5.4), and 6 lipase-related genes (*lipl*). After suppression of each lipase via RNAi, stored lipid droplets were assessed by Oil Red O staining in fed and fasted adult worms, and the staining intensities in the anterior intestinal region were quantified (Fig. 2A). As shown in Figure 2B and 2C, suppression of *atgl-1* significantly attenuated lipid droplet hydrolysis in the fasted state and substantially increased lipid droplets even in the fed state. Consistently, biochemical triglyceride measurement with total worm extracts showed similar tendencies with Oil Red O staining (Fig. 2D).

The *atgl-1* gene encodes a homolog of mammalian ATGL and has been implicated in the mobilization of fat stores at the dauer stage in *C. elegans* [84]. In accordance with previous reports [105, 106], ATGL-1 is localized at lipid droplets by showing co-localization of ATGL-1::GFP with Nile Red after fixation (Fig. 2E). Compared to feeding, fasting slightly, but not significantly, changed the levels of *atgl-1* mRNA, whereas the mRNA levels of other fasting-

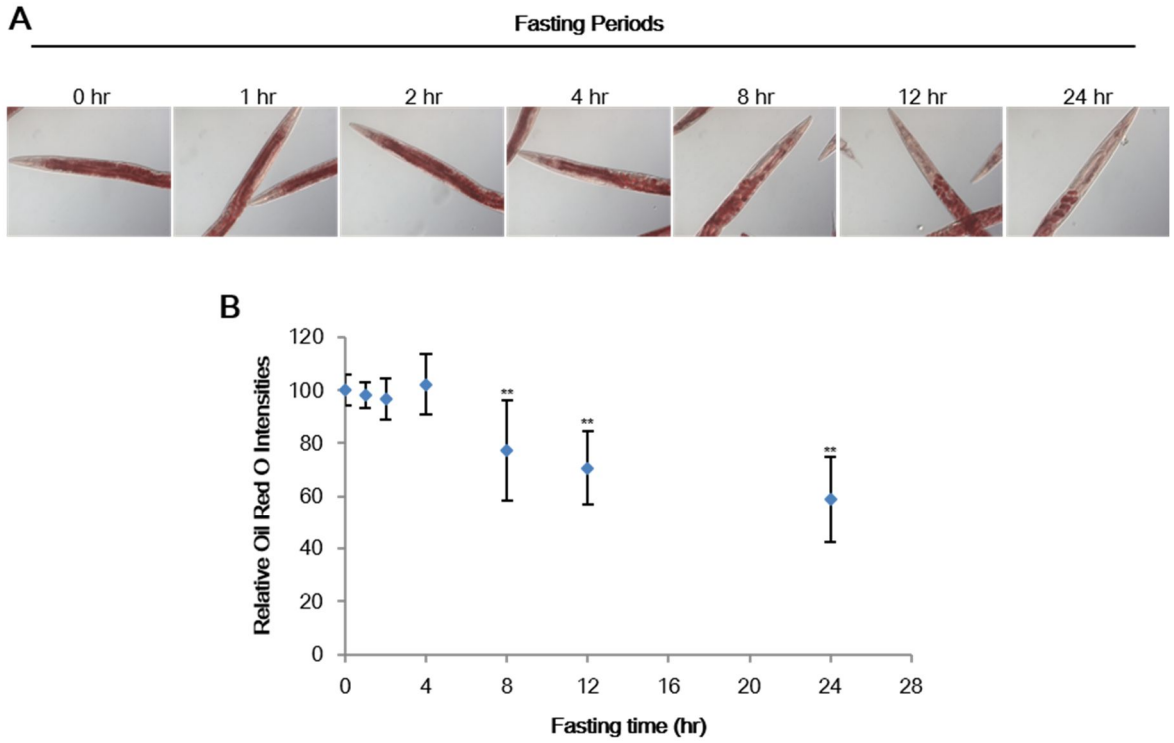

Figure 1. Fasting decreases Oil Red O staining in the anterior intestine.

(A) Representative images and (B) quantitation of Oil Red O intensities. Synchronized young adult-stage worms were fasted in empty plates for the indicated time periods. **, $P < 0.01$ vs. 0-h control, one-way ANOVA.

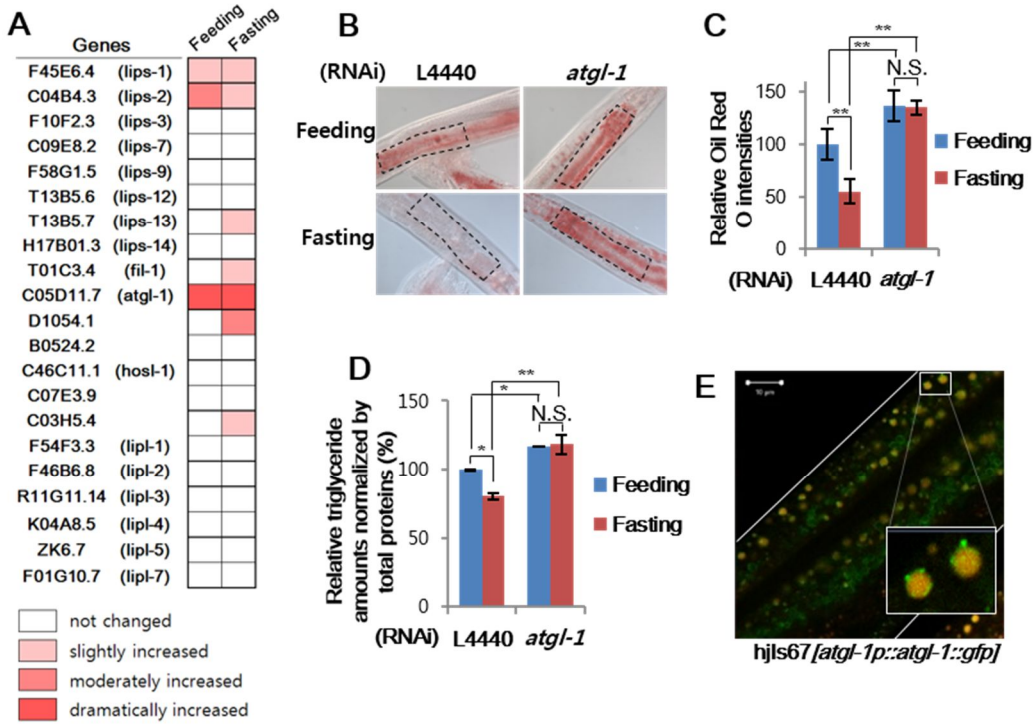

Figure 2. ATGL-1 is a major lipase for fasting-induced lipolysis in *C. elegans*.

(A) RNA interference (RNAi) screening of lipases involved in fasting-induced lipolysis based on Oil Red O staining. Oil Red O staining intensities of young adult worms in the RNAi groups under feeding and 8-h fasting conditions were quantified and classified according to relative fold-increase compared to the L4440 control. (B and C) Representative images and quantitation data of Oil Red O staining with or without *atgl-1* RNAi in young adult worms under feeding and 8-h fasting conditions. Marked areas were subjected to quantitation of Oil Red O staining. (D) Relative triglyceride amounts of young adult worms were measured by biochemical triglyceride assay kit and normalized by total worm extract protein. (E) Confocal microscopic image of *atgl-1(hj67)* worms after fixation and Nile Red staining. Inset is a magnified view. Scale bars, 10 μm. White lines indicate the boundaries of worm bodies. Error bars represent standard deviations. *, $P < 0.05$; **, $P < 0.01$; N.S., not significant.

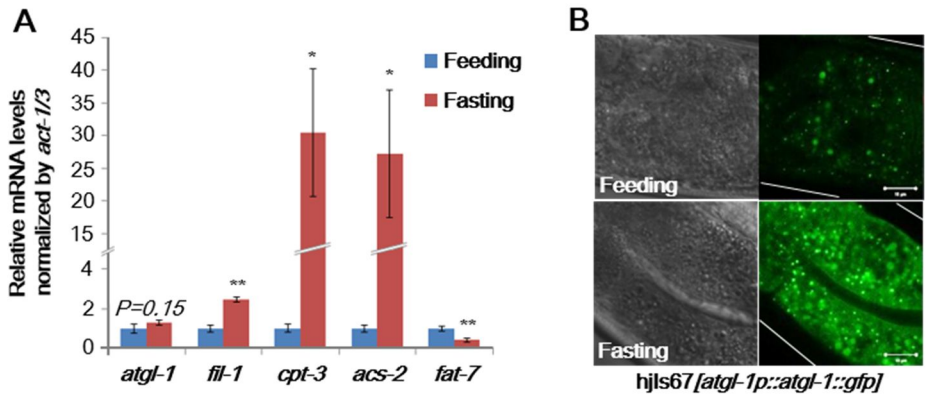

Figure 3. ATGL-1 protein level is increased upon fasting in *C. elegans*.

(A) mRNA levels of *atgl-1* and fasting-responsive genes (*fil-1*, *cpt-2*, *acs-2*, and *fat-7*) measured by qRT-PCR and normalized to *act-1/3* mRNA. (B) Confocal microscopic images of *atgl-1(hj67)* worms under feeding and fasting conditions at the young adult stage. Scale bars, 10 μm. White lines indicate the boundaries of worm bodies. Error bars represent standard deviations. *, $P < 0.05$; **, $P < 0.01$; N.S., not significant.

responsive genes such as *fil-1*, *cpt-3*, *acs-2*, and *fat-7* [73, 97], were altered in fasted worms (Fig. 3A). However, unlike *atgl-1* mRNA, the levels of ATGL-1::GFP protein exhibited an evident increase upon fasting in transgenic worms expressing ATGL-1::GFP (Fig. 3B). These data suggest that post-transcriptional regulations of ATGL-1 would be a key step to mediate the hydrolysis of stored lipid metabolites in fasted worms.

LID-1 is a lipid droplet protein in *C. elegans* homologous to mammalian CGI-58

While *C. elegans* conserves *atgl-1* similar to other eukaryotes, it does not have the lipid droplet binding protein perilipin (Fig. 4). In mammals, CGI-58, which belongs to esterase/lipase/thioesterase subfamily, is a lipid droplet associated protein essential for ATGL activation. *C. elegans* has three genes, C25A1.12, C37H5.2, and C37H5.3, which show sequence homology with mammalian CGI-58/ABHD5 (Fig. 5A). To identify an ortholog of mammalian CGI-58, I examined which *C. elegans* gene(s) would preserve a unique character of CGI-58 family, a loss of active serine at GXSXG motif in α/β hydrolase domain [28, 107]. As shown in Figure 5B, the serine residue of the GXSXG motif is substituted to alanine only in C25A1.12, but not in C37H5.2 and C37H5.3. These results suggest that C25A1.12 (named as *lid-1*) might be an ortholog of CGI-58 whereas C37H5.2 and C37H5.3 might be hydrolase proteins. The amino acid sequence of *lid-1* shares approximately 40% identity with mammalian CGI-58 (Fig. 5C).

To characterize the roles of LID-1 in *C. elegans*, I generated transgenic worms expressing LID-1::GFP in the intestinal cells. In live worms, LID-1::GFP explicitly formed ring-like structures on the surface of lipid droplets, which was confirmed by co-staining with Oil Red O or Nile Red after fixation (Fig. 5D). These data suggest that LID-1 is a genuine lipid droplet protein in *C. elegans*. However, the subcellular distribution of Nile Red staining without

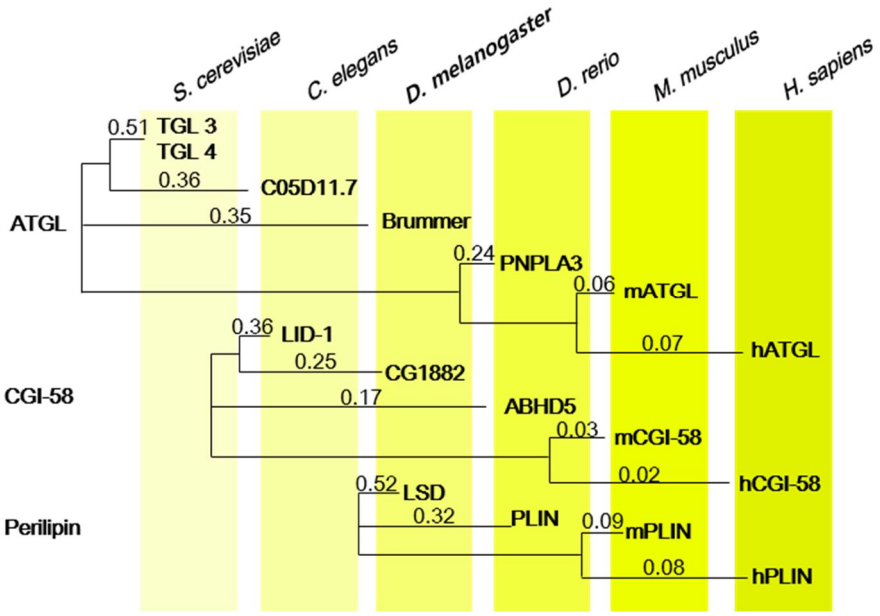

Figure 4 ATGL and CGI-58, not perilipin, are conserved in *C. elegans*.

Phylogenic trees of ATGL, CGI-58, and Perilipin. Amino acid sequences of each gene were subjected to multiple alignments and analyzed for phylogenic trees using ClustalW. Trees were modified for species grouping, and the number indicated on each branch denotes the branch length. Trees and branch lengths were obtained by neighbor joining method.

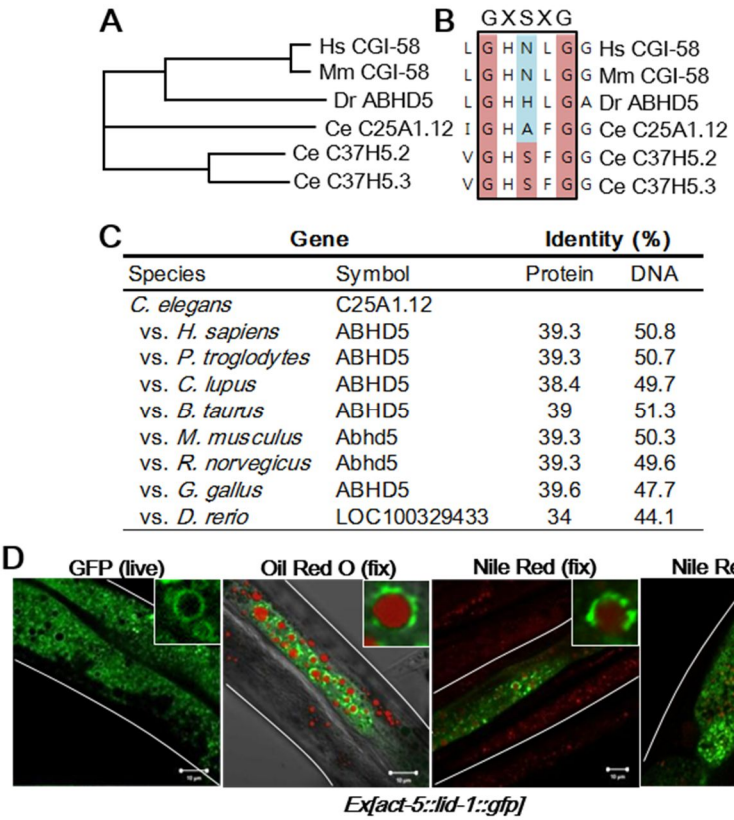

Figure 5. *lid-1*, C25A1.12, is a homolog of CGI-58 and localizes to lipid droplets.

(A) Phylogenic trees of CGI-58 gene family members on the basis of amino acid sequences from *Homo sapiens* (Hs), *Mus musculus* (Mm), *Dario rerio* (Dr), and *Caenorhabditis elegans* (Ce). Amino acid sequences of each gene were subjected to multiple alignments and analyzed for phylogenetic trees obtained by neighbor joining method using ClustalW. (B) Alignment of the GXSXG motif in the α/β hydrolase domain of CGI-58 gene family. (C) Homology scores of LID-1 (C25A1.12) obtained from the Homologene database. (D) Confocal images showing the localization of GFP-fused LID-1 in live worms and in fixed worms co-stained with Oil Red O and Nile Red. The stained area of the Oil Red O image is pseudocolored red. Insets are magnified views. Scale bars, 10 μm. White lines indicate the boundaries of worm bodies.

fixation in live worms was distinct from that of LID-1::GFP, implying that LID-1-containing lipid droplets may be different from lysosome-related organelles (Fig. 5D).

LID-1 is required for ATGL-1 function

The finding that mammalian CGI-58 is dispersed in cytoplasm upon lipolytic stimuli [29] led us to test whether fasted worm may change the levels of *lid-1* mRNA or protein. As shown in Figure 6, fasting did not alter the levels of lid-1 mRNA nor overall distribution of LID-1::GFP. Nevertheless, RNAi of lid-1 prevented the fasting-induced decrease in intestinal lipid droplets of *C. elegans* (Fig. 7A, B). On the contrary, worms treated with RNAi of C37H5.2 or C37H5.3 reduced lipid droplets as wild type worms (Fig. 8), indicating that *lid-1* may have distinct function(s) in fasting condition. Based on these results, I hypothesized that LID-1 is a constitutive lipid droplet protein that may be required for the proper activity of ATGL-1. To elucidate the genetic interaction between the *lid-1* and *atgl-1* genes, I suppressed the *lid-1* gene via RNAi in *atgl-1*-overexpressing worms. Compared to wild-type worms, overexpression of *atgl-1* alone decreased the intestinal lipid droplets in the basal state, whereas RNAi of *lid-1* greatly inhibited the effects of *atgl-1* overexpression on reduction of lipid droplets (Fig. 9A, B). Given that mammalian CGI-58 associates with ATGL [28-30], I next examined whether *C. elegans* LID-1 could interact with ATGL-1. As shown in Figure 9C, LID-1 formed a protein complex with ATGL-1. Furthermore, depletion of *lid-1* via RNAi attenuated the increase in ATGL-1 protein levels and translocation of ATGL-1 into lipid droplets upon fasting (Fig. 9D). These data suggest that in *C. elegans*, LID-1 recruits ATGL-1 to lipid droplets to stimulate lipolysis during fasting.

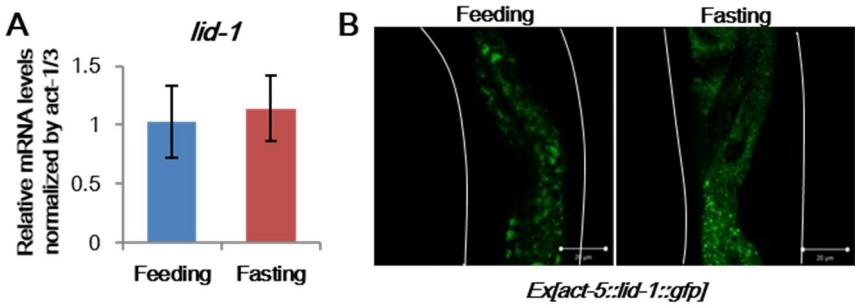

Figure 6. *lid-1* mRNA expression and localization of LID-1::GFP does not change during fasting.

(A) mRNA levels of *lid-1* measured by qRT-PCR and normalized to *act-1/3* mRNA. (B) Young adult-stage *Ex[act-5::lid-1::gfp]* worms were fed or fasted for 8-h and LID-1::GFP distribution was examined. Scale bars, 20 μm.

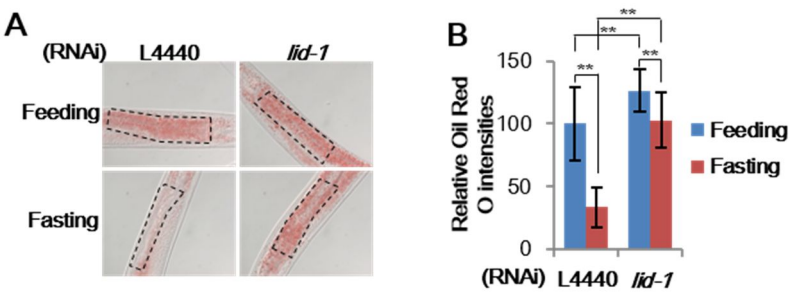

Figure 7. LID-1 is a lipid droplet protein required for fasting-induced lipolysis.

(A and B) Representative images and quantitation data of Oil Red O staining with or without *lid-1* RNAi in young adult worms under feeding or fasting conditions. Marked areas were subjected to quantitation of Oil Red O staining. **, $P < 0.01$; N.S., not significant.

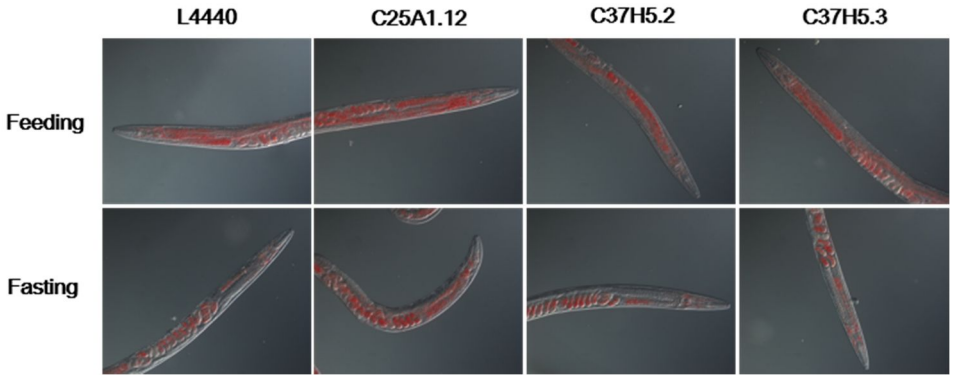

Figure 8. C37H5.2 and C37H5.3 are not required for fasting-induced lipolysis.

Representative images of Oil Red O intensities in young adult worms.

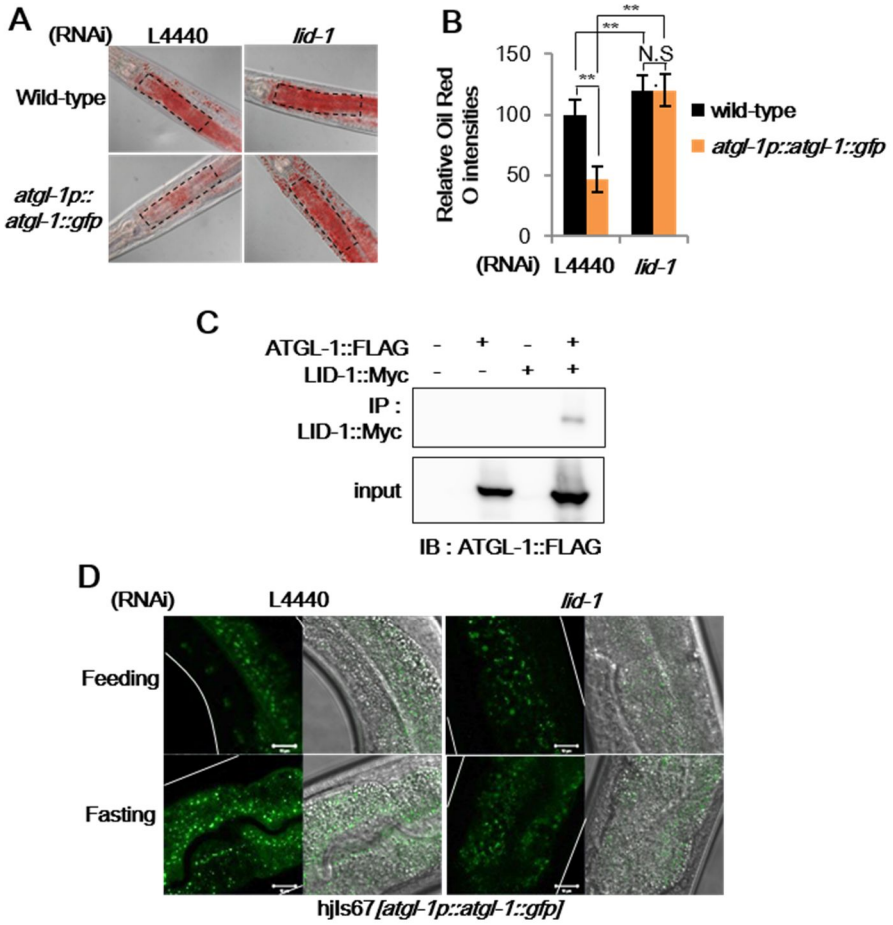

Figure 9. LID-1 is required for ATGL-1 activity.

(A and B) Representative images and quantitation data of Oil Red O staining in *atgl-1(hj67)* worms after L4440 control and *lid-1* RNAi. Marked areas were subjected to quantitation of Oil Red O staining. (C) Co-immunoprecipitation assay of HEK293T cells expressing ATGL-1-Flag and LID-1-Myc. (D) Confocal images of *atgl-1(hj67)* worms under feeding and fasting conditions after L4440 control or *lid-1* RNAi. Scale bars, 10 μm. White lines indicate the boundaries of worm bodies. Error bars represent standard deviations. **, $P < 0.01$; N.S., not significant.

Fasting induces lipolysis via PKA signaling

The observation that in *C. elegans*, ATGL-1 and LID-1 are involved in the hydrolysis of stored lipid droplets upon fasting prompted us to investigate which signaling pathway(s) would be involved in the response to nutritional changes. As key energy sensors, PKA and AMPK have been extensively studied [10, 108], and both these kinases are well-conserved in *C. elegans*. As shown in Figure 10A and 10B, RNAi of *kin-1*, the catalytic subunit of PKA, drastically impaired fasting-induced decrease in lipid droplets. Even under feeding conditions, *kin-1* RNAi substantially elevated intracellular lipid accumulation, as observed in response to *atgl-1* or *lid-1* suppression, implying that these genes are likely involved in the same lipolytic pathway. Because PKA is stimulated by cAMP, I measured whole-body cAMP levels. In fasted worms, cAMP levels were elevated (Fig. 10C). Thus, the *C. elegans* cAMP-PKA pathway appears to be well conserved to reflect energy states throughout evolution. In adult worms, AMPK catalytic subunit mutants [109], *aak-1*(tm1944), *aak-2*(gt33), and *aak-1*(tm1944);*aak-2*(gt33), decreased lipid droplets under fasting conditions (Fig. 11A, B). Consistently, RNAi of *aak-1* and *aak-2* did not suppressed fasting-induced lipolysis (Fig. 11C, D). Compared to wild-type worms, mutations in AMPK exhibited greater decrease of lipid contents upon fasting. These data suggest that in *C. elegans*, PKA is activated upon fasting and plays a critical role in facilitating fasting-induced lipid droplet hydrolysis whereas AMPK signaling may attenuate fasting-induced lipolysis.

To determine whether PKA could indeed modulate the activity of ATGL-1 and LID-1, I tested a *kin-2*, PKA regulatory subunit, mutant strain. *kin-2*(ce179) worms contain a missense mutation (R92C) in the pseudo-substrate domain of the PKA regulatory subunit and thereby exhibit increased PKA activity [110]. Compared to wild-type worms, the levels of accumulated

lipid droplets were greatly decreased in *kin-2*(ce179) worms under well-fed conditions (Fig. 12A, B) A similar phenotype of *kin-2*(ce179) worms was confirmed. by *kin-2* RNAi, indicating t h a t

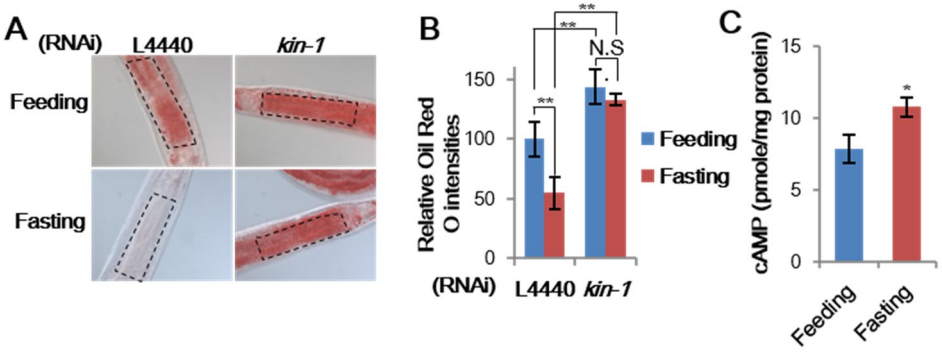

Figure 10. PKA signaling mediates fat mobilization upon fasting in *C. elegans*.

(A and B) Representative images and quantitation data of Oil Red O staining with or without *kin-1* RNAi in young adult worms under feeding or fasting conditions. (C) Cyclic AMP (cAMP) concentrations measured by direct ELISA in total extracts of wild-type worms under feeding and 4-h fasting conditions. . *, $P < 0.05$; **, $P < 0.01$; N.S., not significant.

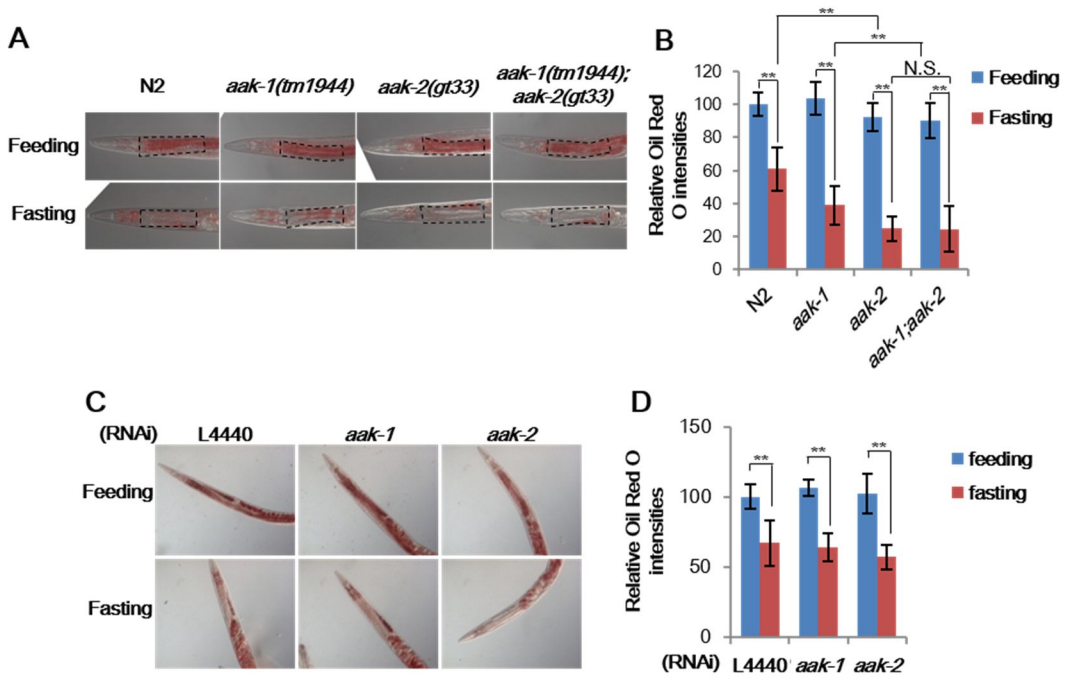

Figure 11. AMPK signaling is not required for fasting-induced lipolysis.

(A and B) Representative images and quantitation data of Oil Red O staining in wild-type and AMPK mutant worms under feeding or fasting conditions (C and D) Representative images and quantitation of Oil Red O intensities with control, *aak-1*, or *aak-2* RNAi in young adult worms under feeding or 8-h fasting conditions. Error bars represent standard deviations. **, $P < 0.01$; N.S., not significant.

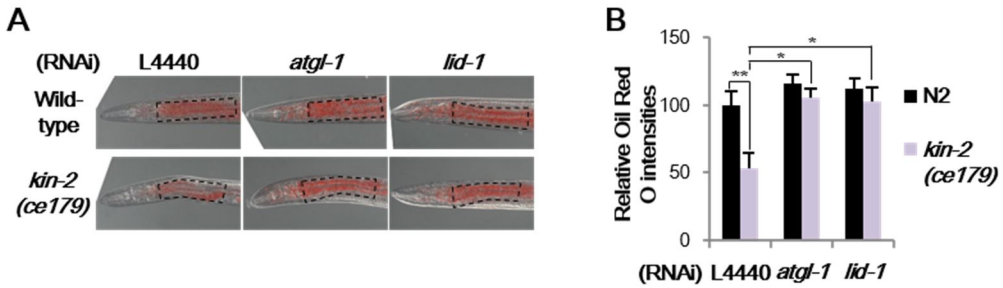

Figure 12. *atgl-1* and *lid-1* act in downstream of PKA signaling.

(A and B) Representative images and quantitation data of Oil Red O staining in the PKA hyperactive *kin-2* mutant strain (*ce179*) after RNAi of *atgl-1* or *lid-1*. For Oil Red O staining, marked areas were subjected to quantitation. Error bars represent standard deviations. *, $P < 0.05$; **, $P < 0.01$; N.S., not significant.

PKA activity seems to be also important for the regulation of lipid metabolism under basal conditions. Intriguingly, in *kin-2*(ce179) worms, knockdown of *atgl-1* and *lid-1* restored the levels of intestinal lipid droplets to nearly those of wild-type worms (Fig. 12A, B). These data suggest that in fasted worms, PKA signaling would act as a key upstream regulator for *atgl-1* and *lid-1*, which may be a central and conserved signaling pathway for lipolysis in most animals upon fasting.

PKA phosphorylates ATGL-1 and enhances protein stability as well as LID-1 binding

Given that PKA acts upstream from ATGL-1 and LID-1 in fasting-induced lipolysis, I asked the question whether PKA might directly phosphorylate ATGL-1 and/or LID-1. Recently, it has been demonstrated that mammalian ATGL is phosphorylated by PKA at multiple sites [33]. In vitro kinase assays revealed that PKA phosphorylated *C. elegans* ATGL-1, but not LID-1 (Fig. 13A, B). A search for PKA phosphorylation site(s) revealed serine 303 of ATGL-1 as one of the potential PKA phosphorylation sites (Fig. 13C). Compared with wild-type ATGL-1, mutation of serine 303 to alanine in ATGL-1 (S303A) abrogated the phosphorylation by PKA, indicating that serine 303 of ATGL-1 is one of the major phosphorylation sites for activated PKA (Fig. 13D).

To gain further insights into ATGL-1 phosphorylation by PKA, I examined localization of ATGL-1::GFP in *kin-2* suppressed worms. Because *kin-2* encodes the regulatory subunit of

PKA, knockdown of *kin-2* increased basal PKA activity in *C. elegans*. It is of interest to note that PKA activation by *kin-2* RNAi or treatment of forskolin, a PKA activator, greatly increased the levels of ATGL-1::GFP intensity, even more than those observed in fasted worms (Fig. 14A, 15A). Moreover, the levels of the *C. elegans* ATGL-1 protein were elevated by forskolin in mammalian cells, whereas the S303A mutation in ATGL-1 attenuated the effect of forskolin

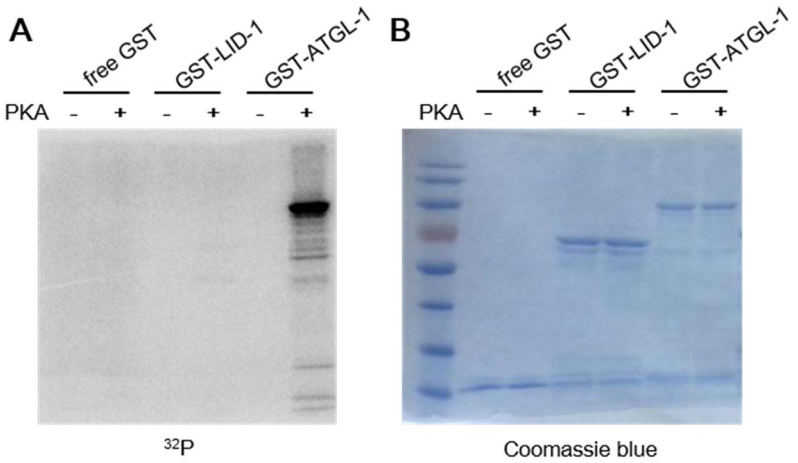

C

Position	Code	Kinase	Peptide	Score
303	S	AGC/PKA	PRMKKRASANALNSF	5.049
316	S	AGC/PKA	SFRTRGESECETCGD	2.530
81	T	AGC/PKA	VSQARSRTFGPLHPE	2.495
303	S	AGC	PRMKKRASANALNSF	2.416
369	T	AGC/PKA	FRLVRYATTAMGISK	2.403

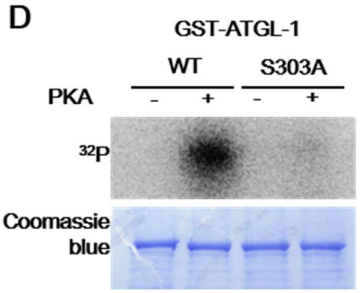

Figure 13. PKA phosphorylates ATGL-1.

(A and B) In vitro kinase assays with recombinant GST-LID-1 and GST-ATGL-1. Purified GST-

fused proteins were incubated with the PKA catalytic subunit and ^{32}P-labeled ATP before SDS-PAGE. After the kinase reaction, proteins were separated by SDS-PAGE and visualized by autoradiography and Coomassie blue staining. (C) Prediction results obtained using the GPS2.1 software were sorted according to the scores indicated. The amino acid sequence of C05D11.7a, an isoform of *C. elegans* ATGL-1, as provided by WormBase, was analyzed using the GPS2.1 software for potential PKA phosphorylation sites. The corresponding kinase was set as AGC/PKA and the threshold as medium. The resulting potential sites were aligned by score and the serine residue with the highest prediction score was selected. (D) In vitro kinase assay with wild-type (WT) ATGL-1 and S303A ATGL-1 recombinant proteins.

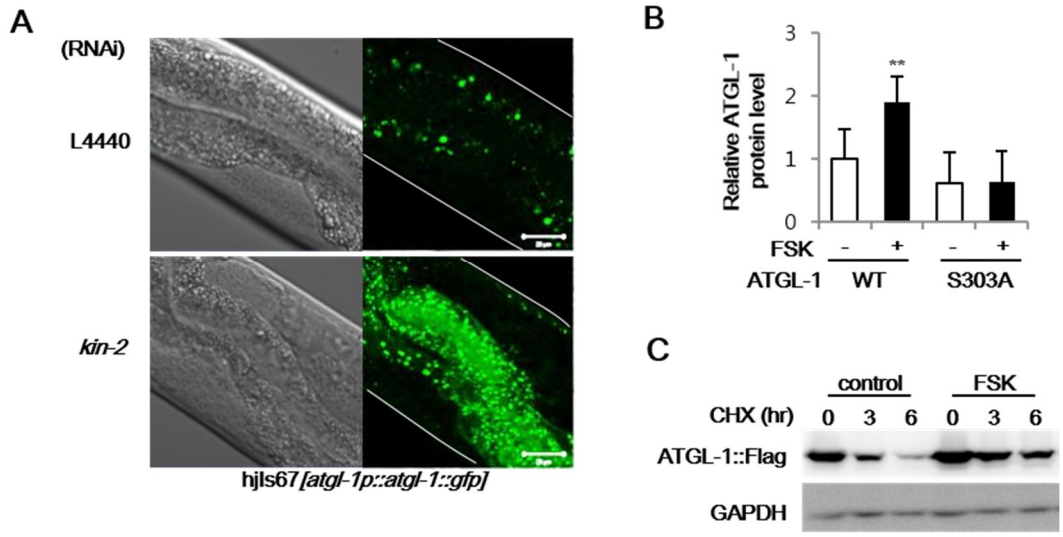

Figure 14. PKA activation increases ATGL-1 protein level.

(A) Confocal images of *atgl-1(hj67)* worms after L4440 control and *kin-2* RNAi. (B) Quantitation of western blots of *C. elegans* ATGL-1 proteins in Cos-1 cells with or without forskolin (FSK; 50 μM, 3-h) treatment. (C) Western blot data of *C. elegans* ATGL-1 proteins in Cos-1 cells treated with cycloheximide (CHX; 50 μg/ml). Forskolin (FSK; 50 μM) was pre-treated for 3-h. GAPDH was used as a loading control. Scale bars, 20 μm. White lines indicate the boundaries of worm bodies. Error bars represent standard deviations. **, $P < 0.01$.

(Fig. 14B). In addition, forskolin treatment enhanced the stability of ATGL-1 protein (Fig 14C). Because *atgl-1* mRNA levels were not significantly altered upon fasting (Fig. 3A), I investigated whether the increase in ATGL-1 protein by PKA was modulated by protein stability. To test this, worms were treated with MG132, a proteasome inhibitor, and the levels of the ATGL-1::GFP protein were monitored. As shown in Figure 15A, the inhibition of proteasomal degradation with MG132 augmented the levels of ATGL-1::GFP. Furthermore, MG132 treatment did not further elevate ATGL-1::GFP level in forskolin treated worms. Next, I asked the question whether phosphorylation of ATGL-1 by PKA may affect LID-1 binding. As shown in Figure 15B, PKA activation with forskolin evidently potentiated the interaction between ATGL-1 and LID-1, which was drastically attenuated in ATGL-1 S303A mutant. In addition, inhibition of PKA signaling by *kin-1* RNAi sufficiently blocked the increase of ATGL-1::GFP signal upon fasting (Fig. 15C). Taken together, these data suggest that ATGL-1 phosphorylation by PKA stimulates the levels of ATGL-1 protein via inhibition of proteasomal degradation and/or promoting LID-1 binding.

Lipid hydrolysis is required for energy production during fasting

In general, ATP production via fatty acid oxidation demands more oxygen. To examine the roles of ATGL-1 and LID-1 in energy production during fasting, I measured oxygen consumption rate as an index of fatty acid oxidation activity. Fasted worms consumed more

oxygen, presumably due to increased mitochondrial activity to oxidize lipid metabolites, as previously reported [97]. Inhibition of lipolytic pathways by RNAi of *atgl-1* or *lid-1* alleviated the fasting-induced increase in oxygen consumption rate (Fig. 16A). These data indicate that hydrolysis of stored lipids by *atgl-1* or *lid-1* would eventually lead to an energy-producing process such as fatty acid oxidation.

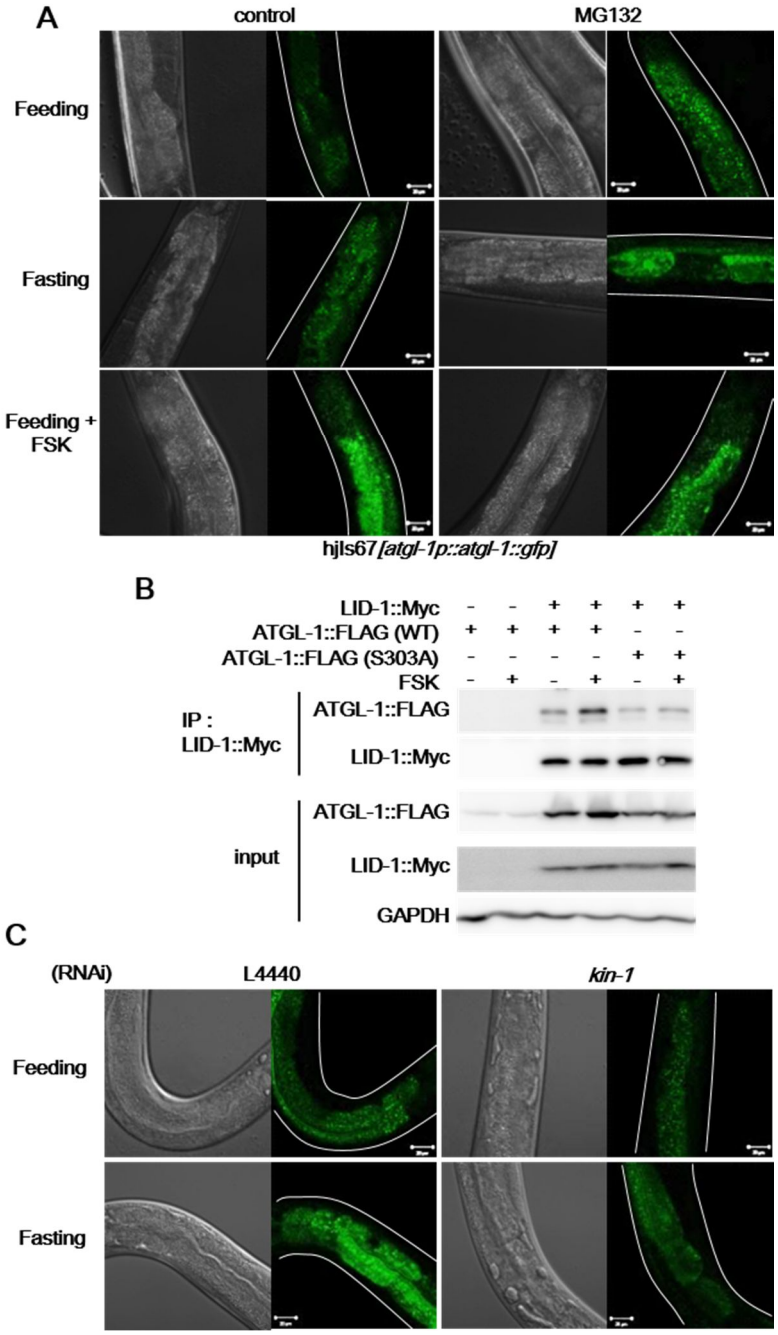

Figure 15. PKA regulates ATGL-1 protein stability as well as LID-1 binding.

(A) Confocal images of *atgl-1(hj67)* worms treated with DMSO, forskolin (FSK; 100 μM) or MG132 (100 μM) under feeding or fasting condition. (B) Co-immunoprecipitation assay of Cos-1 cells expressing ATGL-1-Flag and LID-1-Myc in the absence or presence of forskolin (FSK; 50 μM, 3-h). (C) Confocal images of *atgl-1(hj67)* worms after L4440 control and *kin-1* RNAi under feeding or 4-h fasting conditions. Scale bars, 20 μm. White lines indicate the boundaries of worm bodies.

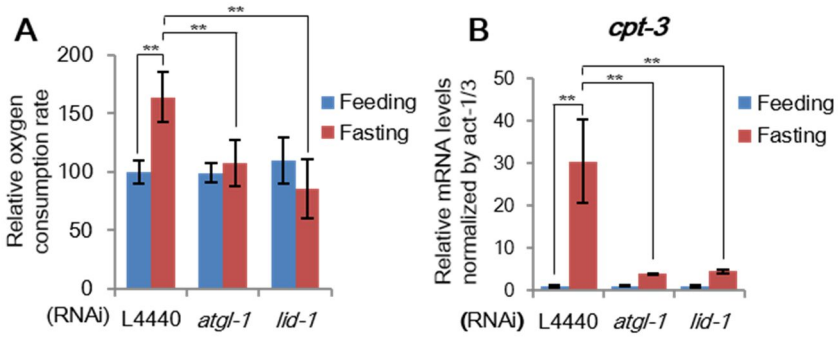

Figure 16. *atgl-1* and *lid-1* are required for energy production during fasting.

(A) The oxygen consumption rates of worms in oxygen-saturated M9 buffer after feeding and fasting, normalized to the amounts of total proteins. For details, see Materials and Methods. (B) mRNA levels of *cpt-3* measured by qRT-PCR and normalized to *act-1/3* mRNA. Error bars represent standard deviations. **, $P < 0.01$.

To determine the effects of *atgl-1*, *lid-1*, and *kin-1* RNAi on gene expression upon fasting, I performed microarray analyses to identify fasting-responsive gene sets. Gene set enrichment analysis using DAVID showed that various signaling pathways, including fatty acid and nutrient metabolic pathways, were significantly altered upon fasting (Table 1). Clustering analysis and gene expression profiles also revealed that disruption of PKA signaling dampened fasting-induced gene expression changes, implying that PKA could mediate pleiotropic responses (Fig. 17). By contrast, the global expression patterns of the *atgl-1* and *lid-1* RNAi groups were not very different from that of the control group (Fig. 17). On the other hand, qRT-PCR analysis showed that changes in mRNA levels of genes involved in fatty acid oxidation, such as *cpt-3*, were blunted by RNAi of *atgl-1* and *lid-1* (Fig. 16B). These data suggest that the functions of both *atgl-1* and *lid-1* are more closely and selectively associated with lipolytic pathways and fatty acid oxidation downstream from PKA.

Table 1. Gene set enrichment analysis of fasting-responsive genes

Genes exhibiting greater than 1.5-fold change in microarray experiments were selected for DAVID analysis. The EASE score represents statistical significance of enrichment and the count represents the number of genes enriched in the indicated KEGG pathway categories.

KEGG Pathway Term	EASE Score	Count
Lysosome	2.805E-08	44
Wnt signaling pathway	4.863E-06	46
Fatty acid metabolism	1.872E-05	44
Valine, leucine and isoleucine degradation	0.0001072	31
MAPK signaling pathway	0.000293	42
TGF-beta signaling pathway	0.0017474	25
Tryptophan metabolism	0.0025923	23
Propanoate metabolism	0.0027735	20
Biosynthesis of unsaturated fatty acids	0.0167111	11
beta-Alanine metabolism	0.0190041	14
Sphingolipid metabolism	0.0190041	13
Calcium signaling pathway	0.0232046	22
Glycine, serine and threonine metabolism	0.0258394	13
Glycolysis / Gluconeogenesis	0.030508	29
ErbB signaling pathway	0.0306392	26
Butanoate metabolism	0.0307024	19
Fatty acid elongation in mitochondria	0.0310375	10
alpha-Linolenic acid metabolism	0.0426195	7
Lysine degradation	0.0498556	18
Drug metabolism	0.0535186	26
Limonene and pinene degradation	0.0719449	13
Jak-STAT signaling pathway	0.0975159	12

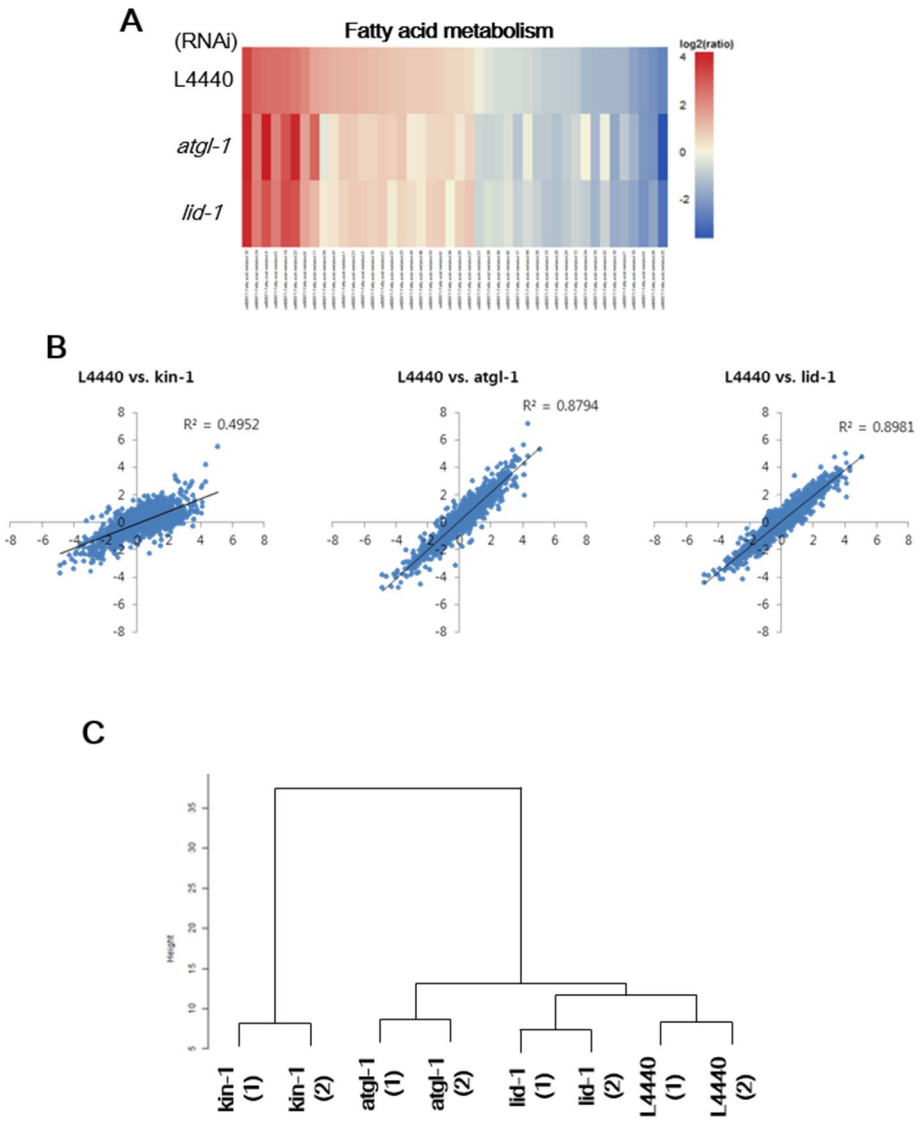

Figure 17. RNAi of *atgl-1* or *lid-1* does not alter genome-wide gene expression upon fasting.

(A) Heat map of fasting-responsive genes that are categorized into fatty acid metabolism by DAVID analysis. (B) Correlation analysis of microarray data. Fold-changes in gene expression upon fasting in each RNAi group were obtained and analyzed. The *x*-axes denote fold-changes in L4440 fasting vs. L4440 feeding, and the *y*-axis denotes fold-change in the *kin-1*, *atgl-1*, or *lid-1* group fasting vs. feeding. Each dot indicates the value for a single gene. Coefficients of determination (R^2) were obtained by linear regression. (C) Clustering analysis of microarray data showing the

similarities between the RNAi groups with respect to fold changes in gene expression upon fasting.

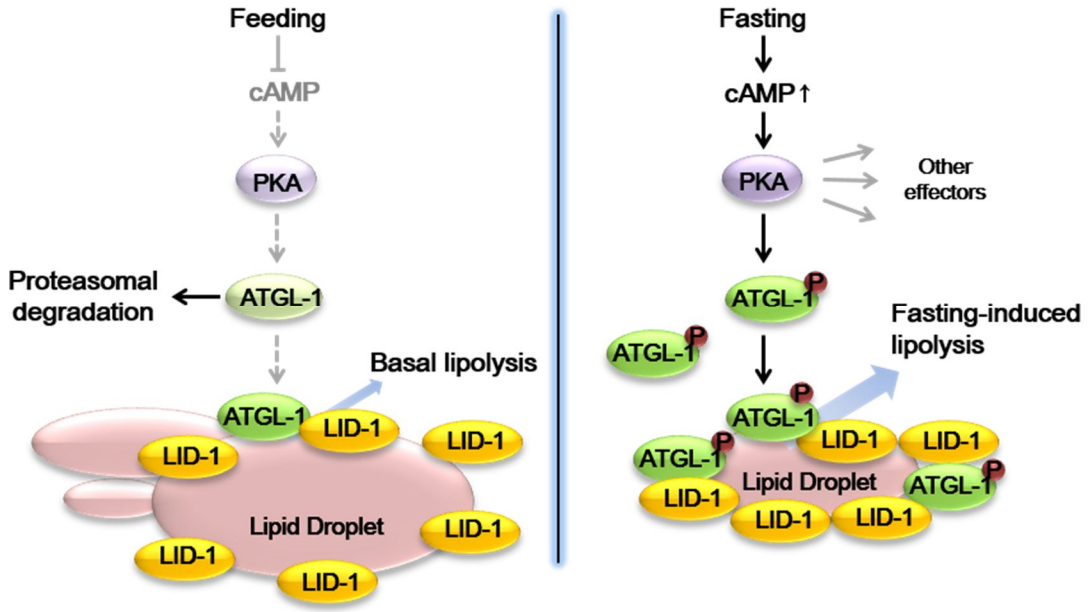

Figure 18. Working model of fasting-induced lipolysis in *C. elegans*.

In the feeding state, ATGL-1 is actively degraded by the proteasome pathway to maintain a low rate of basal lipolysis. In the fasting state, increased cAMP levels activate PKA signaling. Then, PKA phosphorylates and stabilizes ATGL-1, which is recruited to lipid droplets via interaction with LID-1, eventually stimulating lipid hydrolysis.

III-2. Genetic screening for the mediator of PKA-induced lipolysis in *C. elegans*

Protein kinase A system is well-conserved in *C. elegans*

In *C. elegans*, each of the catalytic and regulatory subunit of PKA is encoded by a single gene, *kin-1* and *kin-2*, respectively. To test if *kin-1* and *kin-2* are functionally conserved PKA in *C. elegans*, I performed PKA activity assay upon *kin-1* and *kin-2* RNAi. Knockdown efficiency of each RNAi clones were assessed by qRT-PCR (Fig. 19A). As shown in Fig. 19B, RNAi of *kin-1* significantly decreased PKA activity both in the absence and presence of cAMP. In contrast, RNAi *kin-2* showed increase of basal PKA activity without cAMP. However, in the presence of cAMP, PKA activity of *kin-2* RNAi worm was not different from that of control group. I also observed that addition of PKA inhibitor, PKI, drastically decreased PKA activity. Thus, consistent with previous reports [83, 111], these data have indicated that *kin-1* and *kin-2* in *C. elegans* are functionally well conserved PKA system. And knockdown of PKA subunit genes by feeding RNAi effectively modulate PKA activity in *C. elegans*.

PKA regulates lipid distribution in *C. elegans*

PKA signaling is involved in diverse cellular processes. In *C. elegans*, loss of PKA regulatory subunit, *kin-2*, by RNAi showed pleiotropic phenotypes including short, dumpy morphology with aberrant intestine structure whereas *kin-1* RNAi exhibited relatively normal morphology (Fig 20A). To investigate the changes in lipid metabolisms upon suppression of PKA, I examined lipid storing organelles using lipophilic dyes. It has been reported that staining of lipids in *C. elegans* shows different patterns depending on the properties of lipophilic dyes and fixation process [98, 112]. When worms were stained with Nile Red and fatty-acid-

c o n j u g a t e d

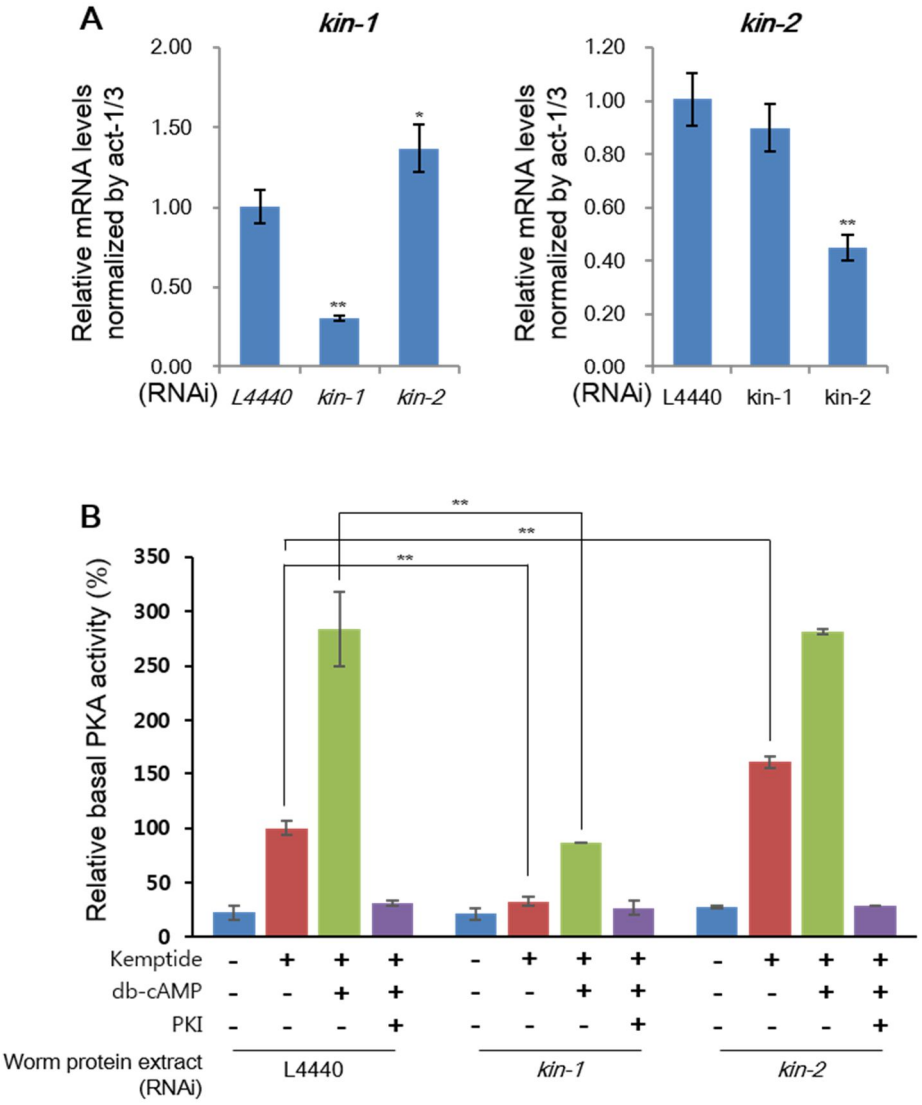

Figure 19. RNAi of *kin-1* and *kin-2* affects basal PKA activity.

(A and B) mRNA levels of *kin-1* and *kin-2* measured by qRT-PCR and normalized to *act-1/3* mRNA. (C) PKA activity assays using the Kemptide substrate and total protein extracts obtained from young adult worms after RNAi in the presence or absence of dibutyryl-cAMP (db-cAMP) and protein kinase A inhibitor peptide (PKI). For details, see Materials and Methods.

Error bars represent standard deviations. *, $P < 0.05$; **, $P < 0.01$.

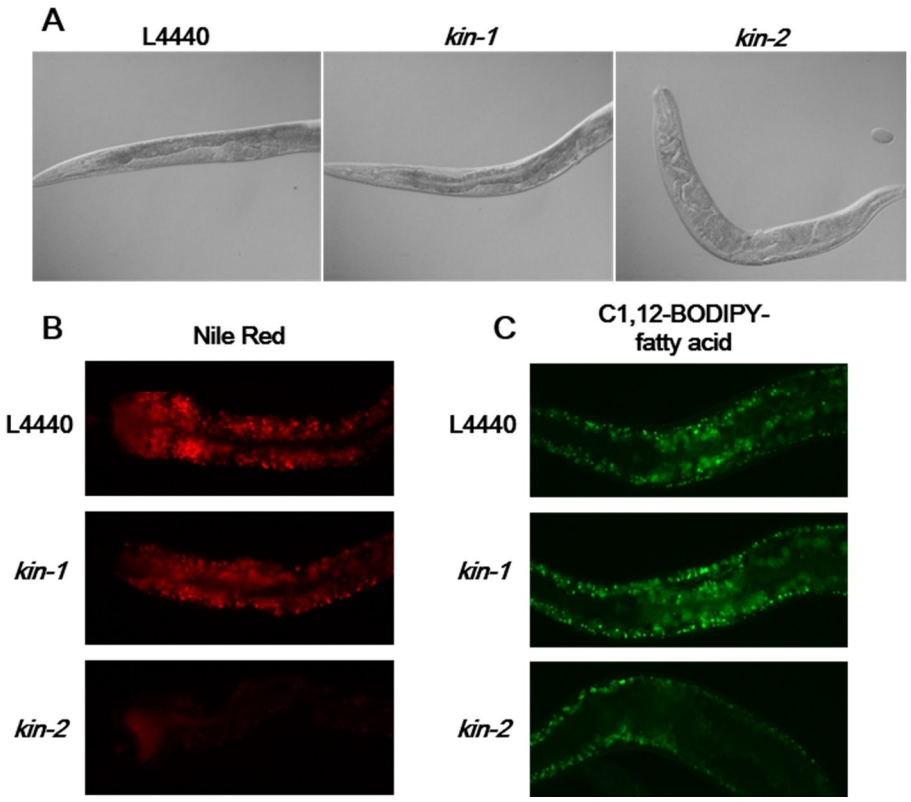

Figure 20. RNAi of *kin-1* and *kin-2* alters morphology and distributions of lipid staining dyes.

DIC image of young adult worms grown on control, *kin-1*, and *kin-2* RNAi plates. (B and C) Fluorescence microscope images of young adult worms with control, *kin-1*, or *kin-2* RNAi stained by Nile Red and C1, 12-BODIPY-fatty acid.

BODIPY under live state, *kin-2* RNAi induced decreased fluorescence intensity in the intestinal cells (Fig. 20B, C). This data suggests that PKA activation can sufficiently decrease lipid storage in Nile Red-stained granules, or LROs, in *C. elegans*. In Oil Red O staining, overall pattern of Oil Red O stained lipid droplets showed increased lipid content in *kin-1* RNAi worms (Fig. 21A), as previously studied (Fig. 10A, B). However, in *kin-2* RNAi group, distribution of Oil Red O stained lipid droplets showed an irregular pattern (Fig. 21A). In *kin-2* RNAi worms, intestinal lipid droplets were greatly reduced (Fig. 21B), and it seemed that lipids were instead ectopically accumulated in extra-intestinal tissues. Intestine tissue-specific lipid reduction by *kin-2* RNAi was also observed in fatty acid-conjugated BODIPY staining, which showed decreased staining intensity in intestine, not in hypodermis (Fig. 20C, 21C). Taken together, these data suggest that PKA signaling could regulate intestinal lipid metabolism in *C. elegans*.

kin-2 RNAi suppressor mutants were isolated by mutagenesis screening

As PKA signaling plays important functions in the regulation of lipid metabolism, I designed random mutagenesis screening to isolate a mediator of PKA-induced lipolysis in *C. elegans*. Synchronized F2 worms obtained from ~18,000 F1 haploid population were screened based on Nile Red staining patterns upon *kin-2* RNAi. Mutant worms that exhibited normal Nile Red intensities were subjected to further investigation. In addition, mutant worms that showed inconsistent *kin-2* RNAi phenotypes or be sterile have been excluded, leaving 9 mutant lines. These mutant lines were tested for RNAi efficiency to further exclude RNAi-defective mutants and three final mutant lines were isolated and considered as *kin-2* RNAi suppressors (Fig. 22).

All isolated *kin-2* RNAi suppressor mutants rescued *kin-2* RNAi phenotypes in terms of Nile Red staining and morphology (Fig. 23A, B). I failed to isolate a mutant that specifically rescues Nile Red phenotype, indicating that these *kin-2* RNAi phenotype might be somehow linked to e a c h

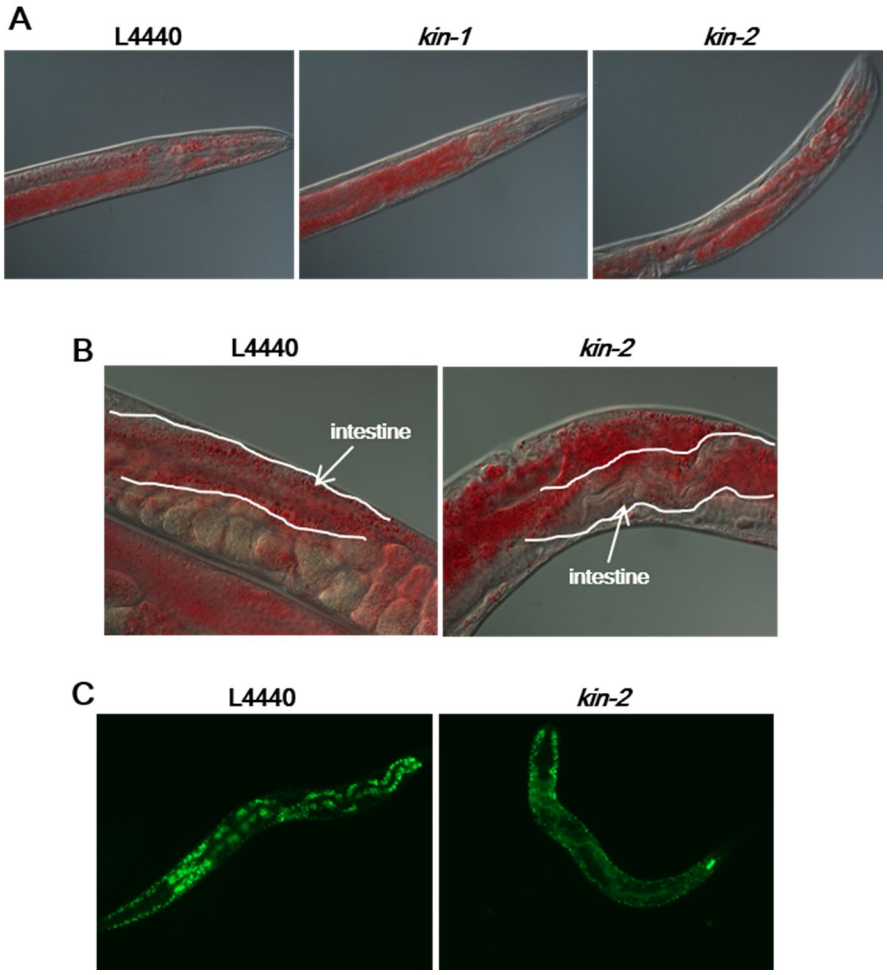

Figure 21. PKA activation depletes intestinal lipid storage.

(A) Representative images of Oil Red O staining in young adult worms after RNAi of *kin-1* or

kin-2. (B) Higher magnification (630x) images of Oil Red O staining of young adult worms after RNAi of *kin-2*. (C) Fluorescence microscope images of young adult worms with control or *kin-2* RNAi stained by C1, 12-BODIPY-fatty acid.

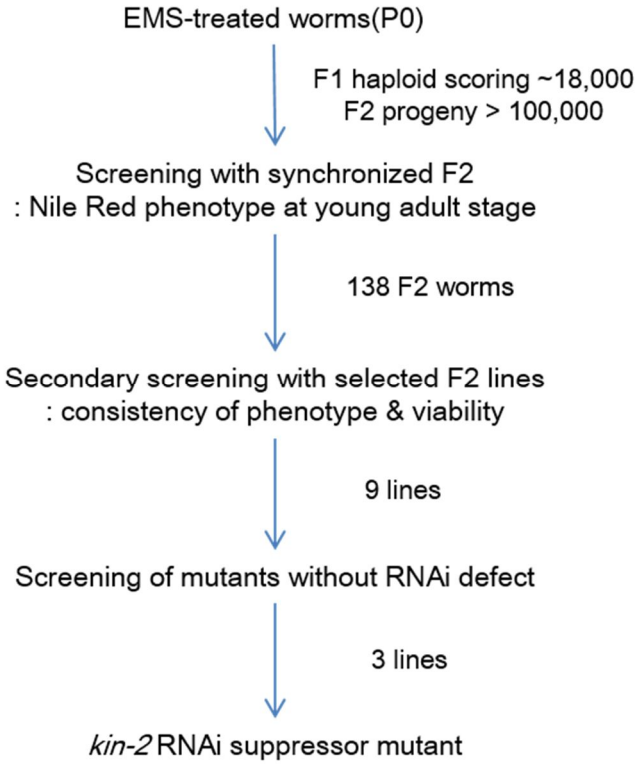

Figure 22. Scheme of *kin-2* RNAi suppressor mutagenesis screening.

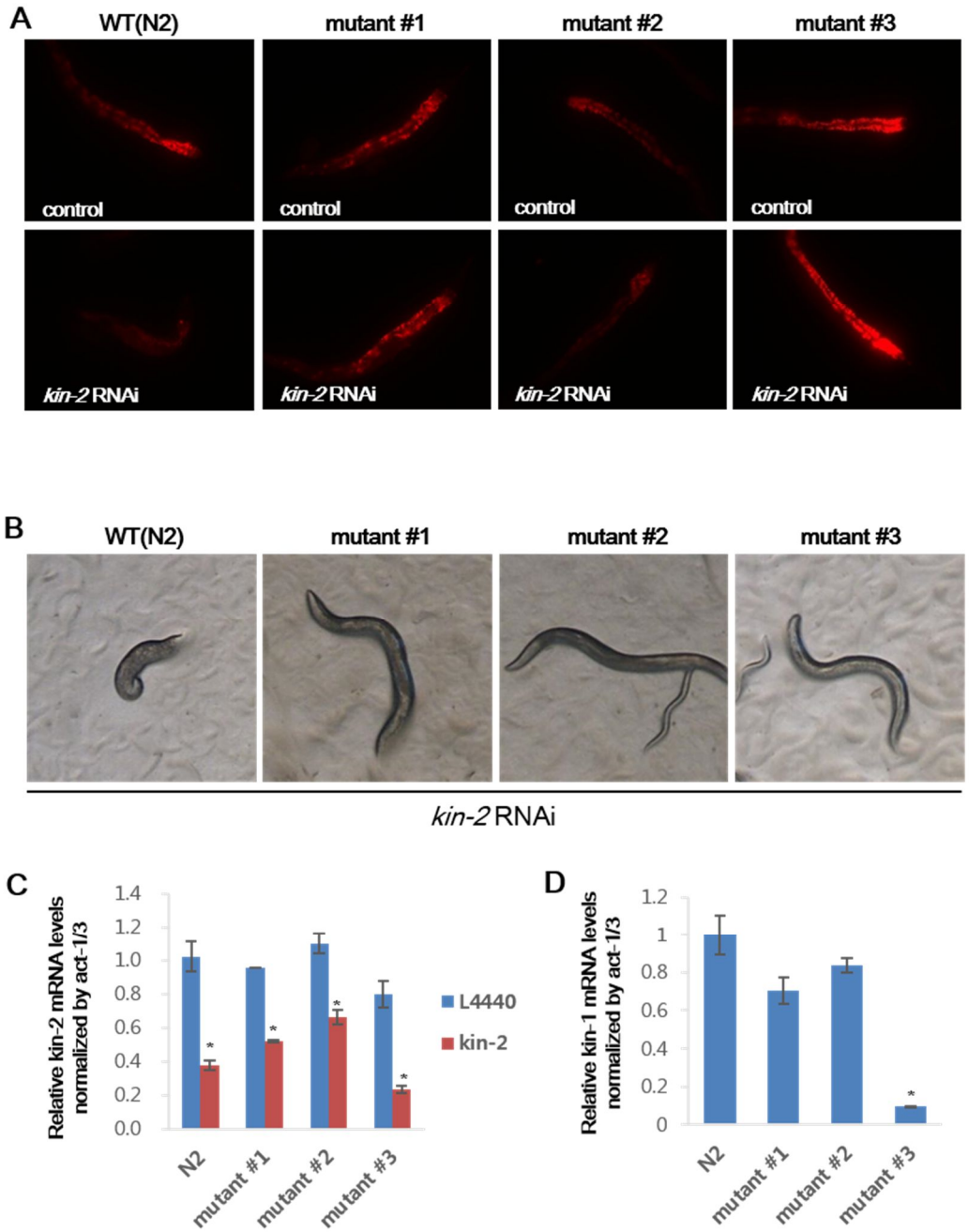

Figure 23. Isolated mutants rescues *kin-2* RNAi phenotypes.

(A) Representative images of Nile Red staining in live mutant worms at young adult stage after RNAi of *kin-2*. (B) Bright-field images of mutant worms at young adult stage grown on *kin-2* RNAi plates. (C) Knockdown efficiencies of kin-2 RNAi in mutant worms as measured by mRNA levels of *kin-2* normalized to *act-1/3* mRNA. (D) mRNA levels of *kin-1* measured by qRT-PCR and normalized to *act-1/3* mRNA. Error bars represent standard deviations. *, $P < 0.05$.

other. Knockdown efficiencies of mutant worms were 40 to 70% (Fig. 23C). Interestingly, mutant #3 showed significantly low levels of *kin-1* expression under basal state, suggesting that the screening process successfully identified mutants associated with PKA pathway (Fig. 23D).

SNP mapping and whole-genome sequencing to identify candidate genes

To identify the genes that were mutated in *kin-2* RNAi suppressor mutants, I first performed SNP mapping. As shown in Tables 2, 3, and 4, SNP mapping data revealed that N2-related markers were enriched in chromosome I for mutant #1, chromosome V for mutant #2, and chromosome III for mutant #3. These results indicate that all the three mutants have different mutations. In addition to SNP mapping, whole-genome sequencing analyses were adopted to identify the genes of interest. However, unexpectedly, whole-genome sequencing showed more than 9,000 strain-specific single nucleotide variations (Fig. 24A), implying that EMS treatment induced a huge number of mutations in *C. elegans* genome. Thus, sequencing data were analyzed based on certain criteria. I selected 1) mutations in SNP mapped chromosome, 2) mutations that are mutant-specific, 3) EMS-induced mutations, and 4) nonsense or missense mutations (Fig. 24B). Through these processes, the number of candidate mutations was cut down to 31 for mutant #1, 44 for mutant #2, and 29 for mutant #3 (Fig. 24C, Table 5).

Table 2. Chromosome mapping result of mutant #1.

SNP profiles of chromosomes were analyzed. N, N2 SNP; C, CB4856 SNP, H, heterologous SNP of N2 and CB4856.

chromosome	genetic position	F2 lines												
		1	2	3	4	5	6	7	8	9	10	11	12	13
I	-20.41	H	H	N	H	C	H	N	N	N	N	H	N	C
	-17.41	H	H	N	H	C	H	N	N	N	N	H	N	C
	-1.03	N	N	N	N	N	N	N	N	N	N	N	N	N
	23.41	H	N	N	N	N	H	N	N	N	H	H	N	N
II	-15.9	N	H	N	H	H	C	N	C	H	C	H	N	H
	1.38	N	C	N	H	H	H	N	C	H	C	H	H	H
	0.11	N	C	N	H	N	H	N	C	H	C	H	H	N
III	-4.13	H	H	N	H	H	N	H	N	H	H	H	H	H
	-0.85	H	H	N	H	H	N	H	N	H	H	H	H	H
	18.04	H	H	N	H	H	N	H	N	H	H	N	H	H
IV	-18.5	H	N	H	H	N	C	C	H	H	C	N	C	C
	-7.28	N	N	H	H	N	H	C	C	H	C	N	H	H
	1.4	H	H	H	H	N	H	C	C	N	C	H	H	H
	5.32	H	H	H	H	N	H	C	C	N	C	H	H	H
	14.55	H	H	H	H	H	C	H	H	N	C	H	C	C
V	-17.65	N	N	C	N	C	C	C	C	H	N	C	C	C
	0.55	H	H	H	N	H	C	N	C	H	N	C	C	C
	16.91	C	H	N	N	N	?	N	?	?	N	C	C	C
X	-18.43	H	H	H	H	C	N	C	C		H	C	H	C
	-0.77	H	H	H	H	H	N	H	H	H	H	H	H	H

Table 3. Chromosome mapping result of mutant #2.

SNP profiles of chromosomes were analyzed. N, N2 SNP; C, CB4856 SNP, H, heterologous SNP of N2 and CB4856.

chromosome	genetic position	F2 lines									
		1	2	3	4	5	6	7	8	9	10
I	-17.41	H	H	N	H	H	H	H	H	H	H
	2.88	N	N	N	C	H	H	H	N	H	H
	23.41	H	H	H	C	H	H	H	C	H	H
II	-15.9	N	H	H	N	H	H	H	H	H	H
	1.38	H	H	H	N	H	H	H	H	H	H
	0.11	N	H	H	N	C	H	H	H	H	C
III	-4.13	H	H	H	H	H	H	H	H	H	H
	-0.85	H	H	H	H	H	H	H	H	H	H
	18.04	H	H	H	N	H	H	H	N	H	H
IV	-18.5	C	H	H	H	H	C	H	H	H	H
	-7.28	C	H	H	C	H	H	H	H	H	H
	1.4	C	H	H	C	H	H	H	H	H	H
	14.55	C	H	H	C	H	C	H	C	C	H
V	-18.57	H	H	H	N	N	H	H	H	H	H
	-17.65	N	H	N	N	N	H	N	H	N	N
	0.55	N	N	N	N	N	N	N	H	N	N
	16.91	H	N	H	H	H	N	H	N	H	H
X	-18.43	H	H	H	N	C	C	H	H	H	N
	-0.77	H	H	H	N	H	H	H	H	H	N
	7.01	H	H	H	N	H	H	H	H	H	H

Table 4. Chromosome mapping result of mutant #3.

SNP profiles of chromosomes were analyzed. N, N2 SNP; C, CB4856 SNP, H, heterologous SNP of N2 and CB4856.

chromosome	genetic position	F2 lines									
		1	2	3	4	5	6	7	8	9	10
I	-17.41	H	N	N	N	H	H	H	H	H	H
	2.88	H	N	N	N	N	H	N	N	N	N
	23.41	H	N	H	H	H	H	H	N	N	C
II	-15.9	N	H	N	C	H	H	H	C	H	H
	1.38	N	H	N	H	H	H	H	H	H	H
	0.11	N	H	N	H	H	N	H	H	H	H
III	-4.13	N	N	N	N	N	H	N	N	H	H
	-0.85	N	N	N	N	N	H	N	N	H	H
	18.04	N	N	N	N	N	N	N	N	N	N
IV	-18.5	C	N	H	H	N	N	N	H	H	C
	-7.28	C	N	H	H	H	H	H	H	H	H
	1.4	C	C	H	H	C	H	H	H	H	H
	14.55	N	N	N	N	N	H	H	H	H	N
V	-18.57	H	N	C	N	C	H	C	C	H	C
	-17.65	H	N	C	N	C	H	C	C	H	C
	0.55	C	N	C	N	C	H	C	C	C	C
	16.91	N	N	C	N	H	N	C	C	H	H
X	-18.43	N	N	H	C	H	H	H	N	H	H
	-0.77	C	N	H	C	H	H	H	H	H	H
	7.01	C	N	H	C	H	H	H	H	H	H

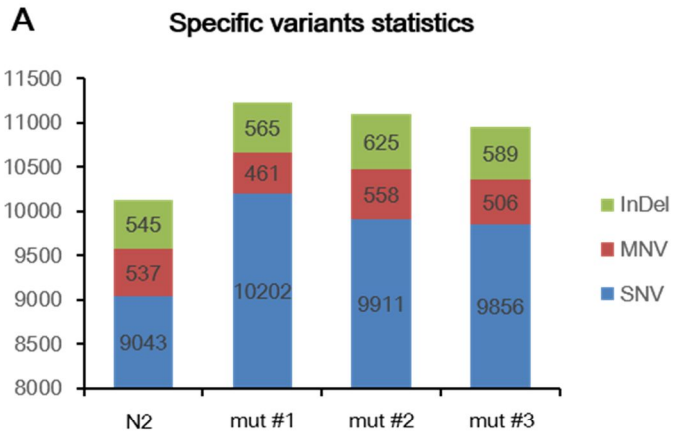

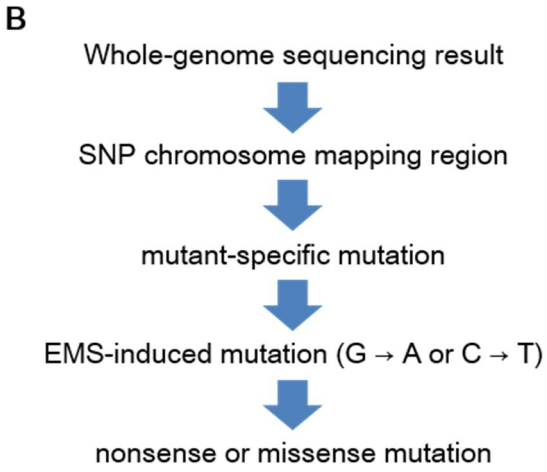

C

	Chromosome	No. of genes with nonsense mutation	No. of genes with missense mutation
mutant #1	I	0	31
mutant #2	V	2	42
mutant #3	III	0	29

Figure 24. Whole-genome sequencing and candidate genes

(A) Total numbers of mutant specific variants observed in whole-genome sequencing. InDel, insertion and deletions; MNV, multinucleotide variants; SNV, single nucleotide variants. (B)

Scheme of selecting candidate genes based on SNP mapping and whole-genome sequencing data. (C) Numbers of candidate gene mutations of each isolated *kin-2* suppressor mutants.

Table 5. List of candidate genes obtained from *kin-2* RNAi suppressor screening

	mutant #1	mutant #2	mutant #3
Candidate genes	Y48G8AR.2 Y71G12B.17 Y54E10A.7 met-1 T21E12.3 gcy-28 sst-20 kin-32 ppw-2 ekl-1 F26A3.5 H05L14.2 kin-10 T08G11.1 F32H2.11 lim-9 hsr-9 daf-16 F55A3.3 png-1 C27C7.7 dnj-27 abt-5 F14B6.4 T09E11.1 K11D2.5 Y18D10A.8 F17B5.1 W09C5.7 Y71A12B.17 ZK337.1	cgp-1 Y39D8B.1 nhr-155 srx-22 T03D3.5 C31B8.8 K08D9.6 T20D4.13 sri-21 nhr-156 oac-24 F14F9.3 K09H11.11 ttn-1 lgc-54 F10D2.10 folt-3 sul-2 ZC178.1 his-49 his-17 oac-50 F21C10.7 F44A2.3 pfk-2 ZK856.12 sma-1 F45D3.4 T07F10.1 F58G11.2 F23B12.7 cyn-7 dhs-23 T26E4.1 srbc-56 T10C6.7 oac-7 sri-65 Y32B12B.4 pus-1 srz-66 Y60A3A.7 clec-261 unc-80	F30H5.3 fbxa-32 Y82E9BR.9 R155.4 Y53G8AM.8 C56G7.2 dnj-16 C28A5.1 nhl-2 T10F2.2 prmt-5 par-3 psf-1 nfm-1 rbf-1 R01H2.2 ogt-1 lpd-7 F10E9.3 ZC262.3 F42H10.2 F44E2.3 F59B2.12 T02C1.2 C07A9.10 mog-1 col-92 col-94 Y79H2A.3

III-3. PKA regulatory subunits and lipolysis in mammalian adipocytes

PKA subunit stoichiometry modulates basal lipolysis

PKA systems in mammals are more complex than in *C. elegans*. In mice, there are 2 catalytic subunit genes and 4 regulatory subunit genes. Tissue distribution of each PKA subunit mRNA shows different patterns (Fig. 25). Catalytic subunit Cα is ubiquitously expressed whereas Cβ is highly expressed in brain. The mRNA expression pattern of regulatory subunit RIα was also ubiquitous although other isoforms showed more tissue-specific pattern. RIβ subunit was highly expressed in brain and low in other tissues. RIIα subunit was enriched in muscle and RIIβ subunit was predominantly expressed in adipose tissue and brain. During adipogenesis, catalytic subunit Cα and regulatory subunit RIIβ expressions were increased (Fig. 26). These data suggest that Cα and RIIβ subunits of PKA might play roles in adipocyte function.

PKA activity is strictly suppressed at basal state and up-regulated upon hormonal changes. I hypothesized that the balance between the amount of regulatory and catalytic subunits of PKA could change basal PKA activity and, consequently, lipolytic activity in adipocytes (Fig. 27). To test this, I transfected siRNA targeting each subunit of PKA into fully differentiated 3T3-L1 adipocytes and measured glycerol release as an indicator of lipolysis. Knockdown efficiencies of each siRNA were examined (Fig. 28). Glycerol release assay showed that knockdown of each PKA subunit alone did not alter lipolysis. Nevertheless, when siRNAs against all the PKA regulatory subunit genes were co-transfected, basal lipolysis rate was significantly increased (Fig. 29). Also, knockdown of both Cα and Cβ showed no difference, implying that PKA activity in adipocytes might be maintained at low level under basal state. These data suggest that alterations in PKA subunit stoichiometry could modulate

lipolysis and that there might be compensatory mechanisms in the function of regulatory subunits in adipocytes.

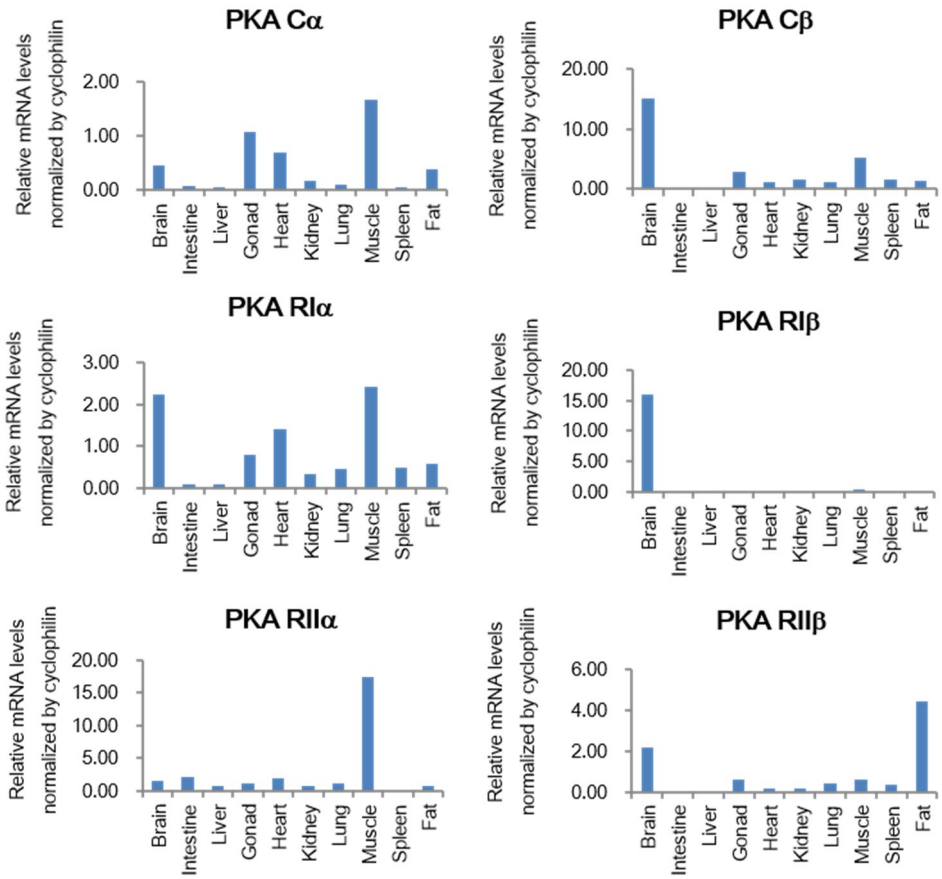

Figure 25. Expressions of PKA subunits are tissue-specific.
mRNA levels of PKA subunit genes measured by qRT-PCR and normalized to cyclophilin mRNA. cyclophilin mRNA level was considered as 1.

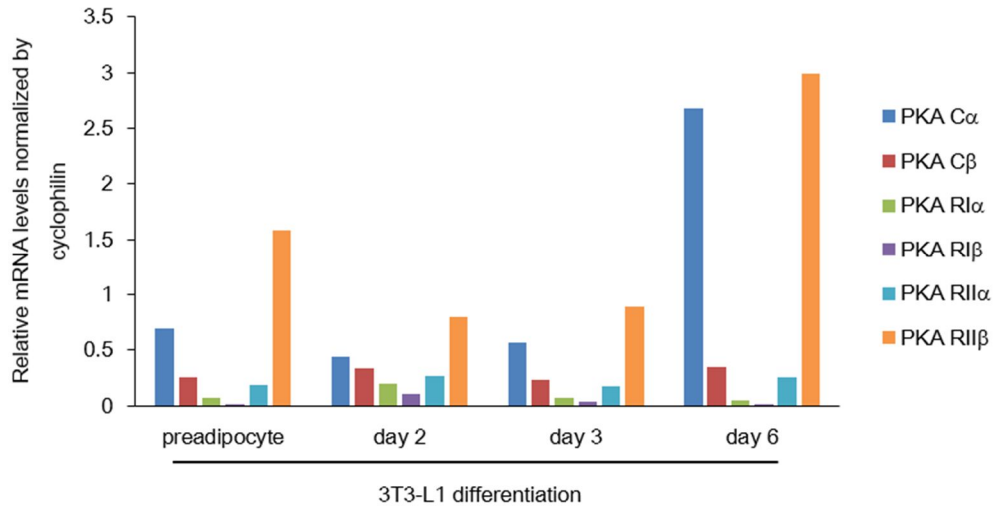

Figure 26. Cα and RIIβ subunits of PKA expressions are increased during adipogenesis. mRNA levels of PKA subunit genes measured by qRT-PCR during the differentiation of 3T3-L1 adipocytes. preadipocytes, day 0 of differentiation media. mRNA levels were normalized to cyclophilin mRNA. cyclophilin mRNA level was considered as 1.

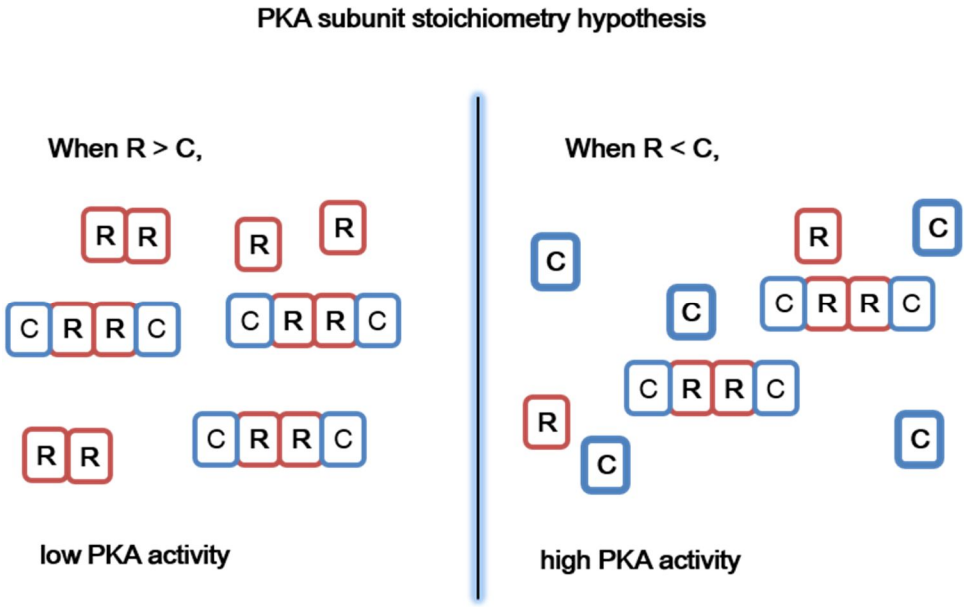

Figure 27. PKA subunit stoichiometry model
At normal state, catalytic subunits (C) of PKA are efficiently suppressed by regulatory subunits (R). When the levels of regulatory subunits of PKA are somehow decreased, catalytic subunits would be de-repressed to activate downstream signaling.

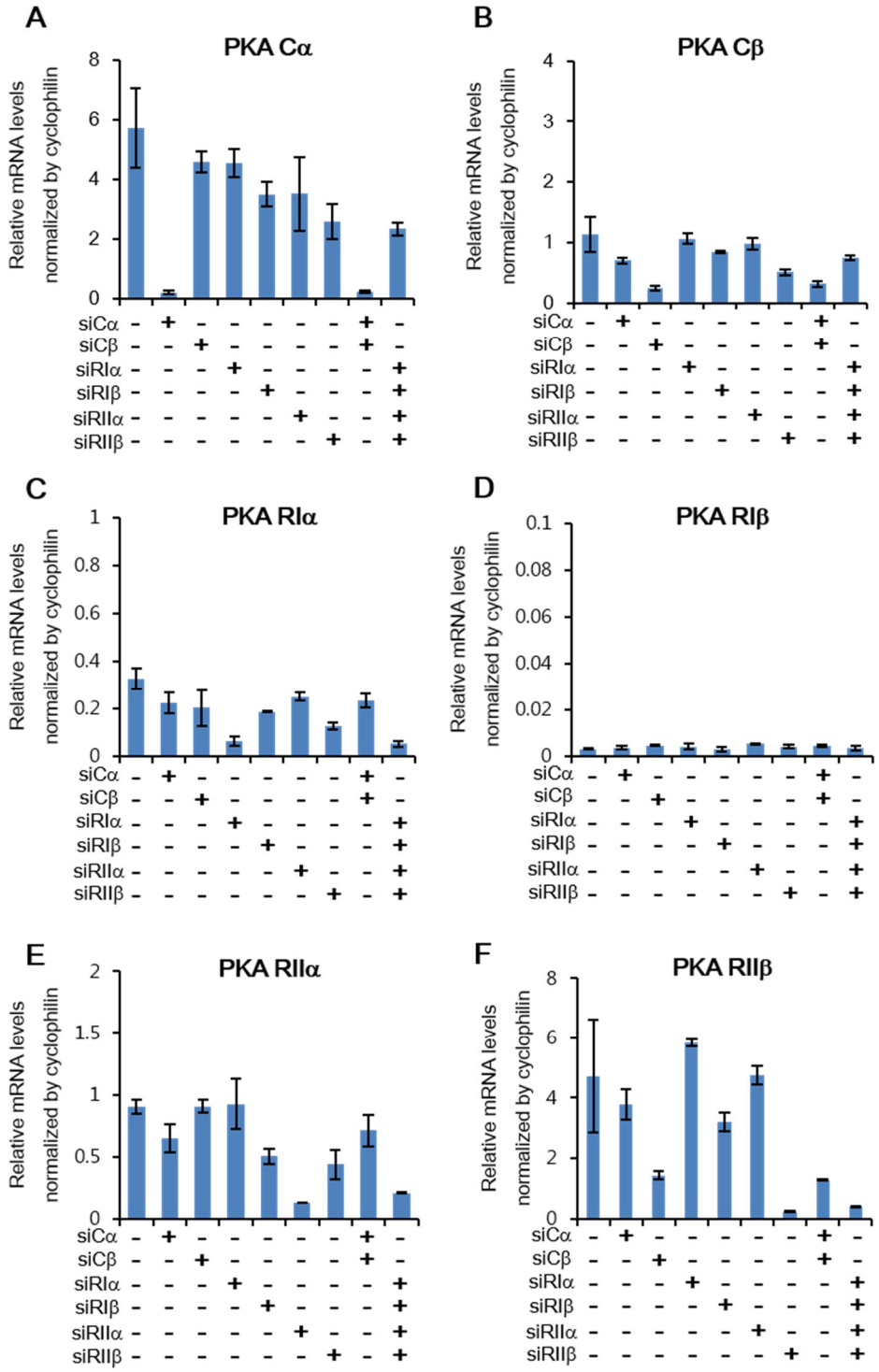

Figure 28. Knockdown efficiencies of siRNAs targeting PKA subunits are confirmed.
(A-F) Knockdown efficiencies of siRNA were confirmed by measuring mRNA levels of PKA subunit genes measured by qRT-PCR and normalized to cyclophilin mRNA. cyclophilin mRNA level was considered as 1. Error bars represent standard deviations.

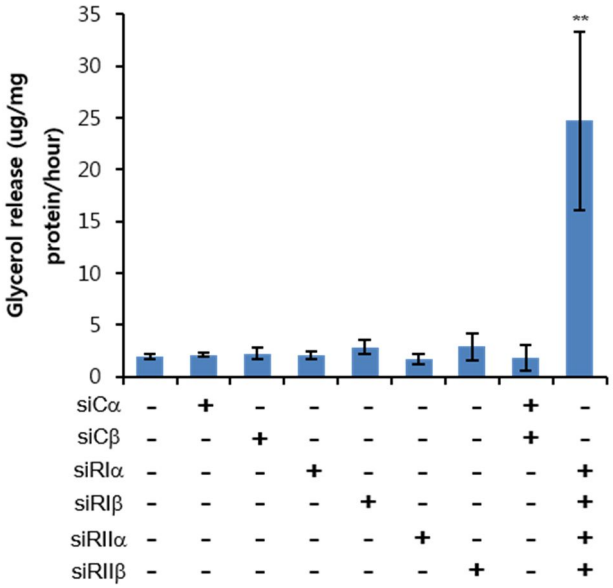

Figure 29. Knockdown of all regulatory subunits of PKA result in increased basal lipolysis in 3T3-L1 adipocytes.

Glycerol concentrations of the media were measured after siRNA transfection and normalized to total protein and time. Error bars represent standard deviations. **, $P < 0.01$ vs. control.

PKA regulatory subunit Iα and IIβ regulates lipolysis and lipid droplets in adipocytes

To identify which isoforms of PKA regulatory subunits are important for the regulation of basal lipolytic activity, I tested the effects of combinationatorial co-transfection of siRNAs in adipocytes. As shown in Figure 30A, I found that without siRNA against RIα or RIIβ, increased glycerol release induced by knockdown of regulatory subunits diminished to basal levels. Furthermore, knockdown of RIα and RIIβ subunits was sufficient to induce lipolysis (Fig. 30B), indicating that these two subunits are indispensable factors in PKA activity control in adipocytes. Also, knockdown of catalytic subunit Cα completely suppressed the effect of RIα and RIIβ regulatory subunit knockdowns (Fig. 30B). In stimulated condition with the treatment of β-adrenergic receptor agonist, isoproterenol, the released glycerol levels were not affected by knockdown of RIα or RIIβ subunits (Fig. 30C).

Consistent with the glycerol release data, siRNA transfection targeting PKA regulatory subunits leads to great reduction of lipid droplets in adipocytes (Fig. 31A, B). Also, knockdown of RIα and RIIβ subunits was sufficient to decrease lipid droplet contents (Fig. 31C). Furthermore, the knockdown effect of regulatory subunits was fully suppressed by knockdown of catalytic subunits (Fig. 31D). The mRNA expressions of genes involved in lipid metabolism were also altered by PKA subunit imbalance. Suppression of regulatory subunits with siRNA significantly decreased perilipin 1 mRNA, which might be associated with lipid droplet reduction (Fig. 32A). ATGL and HSL expressions were decreased by 50% whereas CGI-58 expression was increased (Fig. 32B). Interestingly, the mRNA levels of lipogenic genes including SREBP1c, FAS, and SCD1 were decreased (Fig 32C). In correlation with the glycerol release and lipid droplet staining data, gene expression changes induced by knockdown of regulatory subunits were rescued by suppression of catalytic subunits. These data suggest the

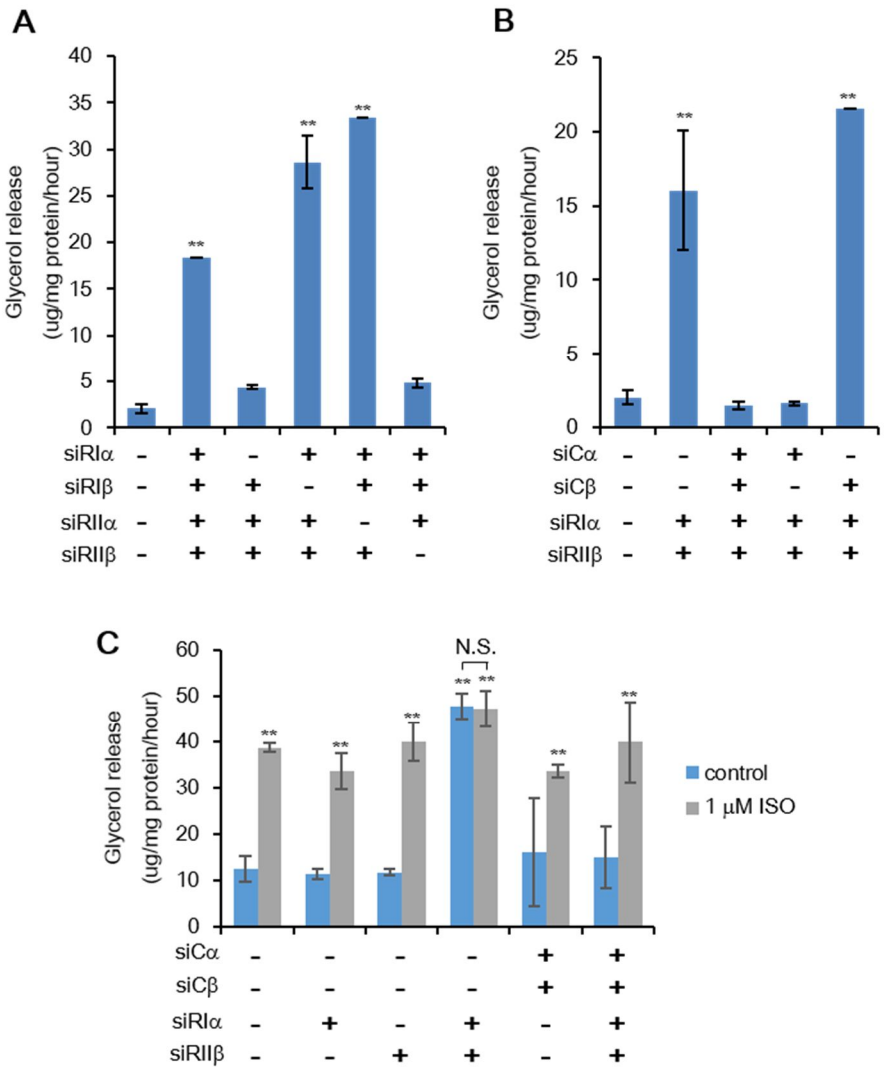

Figure 30. RIα and RIIβ subunits are necessary and sufficient factors for maintaining basal lipolysis.

(A and B) Glycerol concentrations of the media from fully differentiated 3T3-L1 adipocytes were measured after siRNA transfection and normalized to total protein and time. (C) Glycerol concentrations of the media from fully differentiated 3T3-L1 adipocytes in the presence or absence of 1 μM isoproterenol (ISO). Glycerol concentrations were normalized to total protein and time. Error bars represent standard deviations. **, $P < 0.01$ vs. control; N.S., not significant.

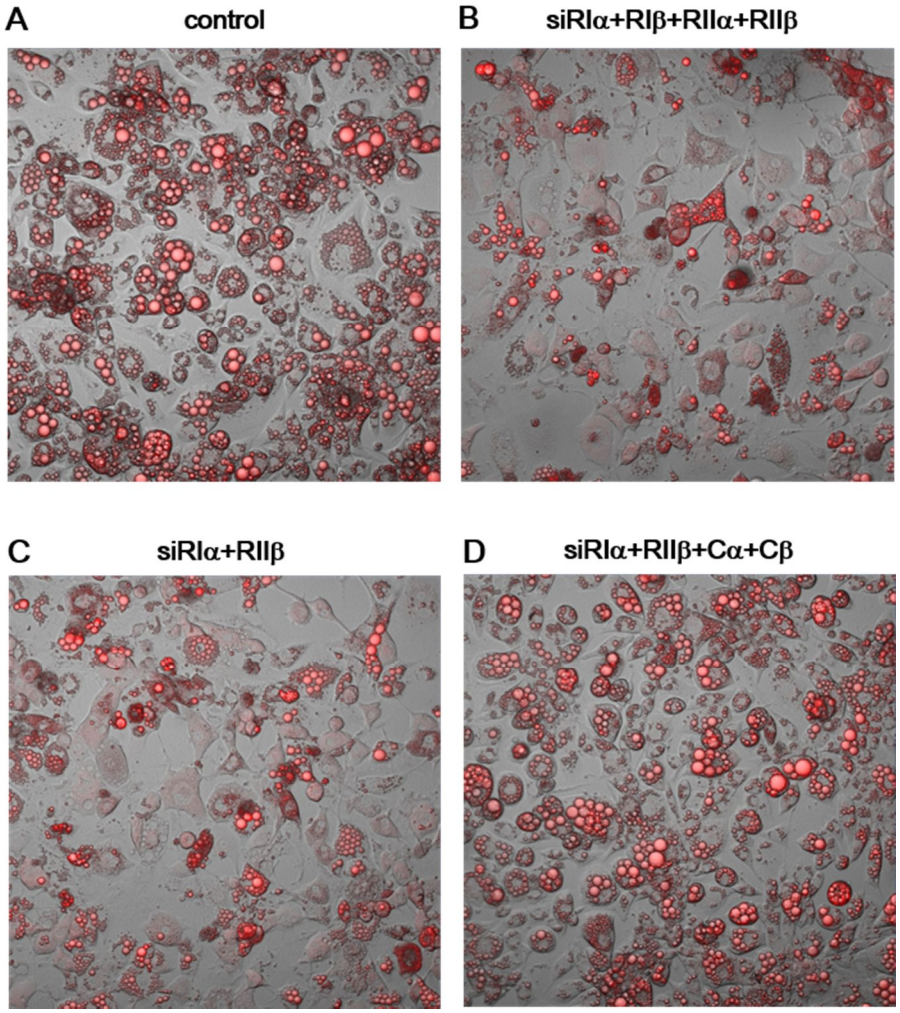

Figure 31. Knockdown of PKA regulatory subunits depletes lipid droplets in adipocytes. (A-D) Nile Red staining images merged with DIC of fully differentiated 3T3-L1 adipocytes 48 hours after siRNA transfections.

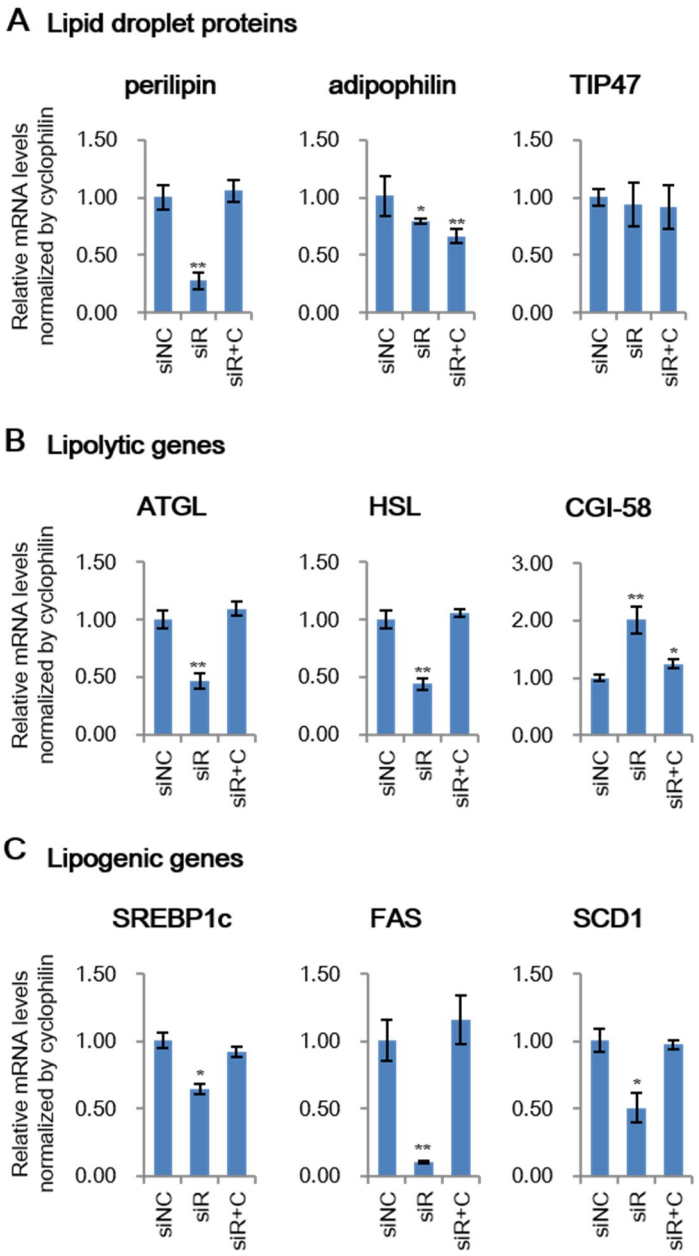

Figure 32. Knockdown of PKA regulatory subunits changes lipid metabolism gene expressions.

(A-C) mRNA levels of lipid droplet proteins, lipolytic genes and lipogenic genes were measured in fully differentiated 3T3-L1 adipocytes 24 hours after siRNA transfection (siNC, negative control; siR, siRIα+RIIβ: siR+C, siRIα+RIIβ+Cα+Cβ). mRNA levels were normalized to cyclophilin mRNA. Error bars represent standard deviations. *, $P < 0.05$; **, $P <$

0.01 vs. siNC control.

subunits in the cell-autonomous regulation of lipolysis and maintenance of lipid droplets in adipocytes, which is primarily mediated by PKA activity.

ATGL is required for PKA-mediated lipolysis

Next, I questioned which lipase is involved in the increased lipolysis by knockdown of PKA regulatory subunits. Co-transfection of siRNA against ATGL and HSL revealed that suppression of ATGL partially decreased lipolysis while knockdown of HSL did not (Fig. 33A). Reduction of lipid droplets due to suppression of PKA regulatory subunits was not fully rescued by knockdown of ATGL, possibly, due to the incomplete suppression of lipolysis (Fig. 33B). These results indicate that ATGL would be the major lipase that mediates lipolysis induced by PKA subunit imbalance.

To further investigate the mechanisms of PKA-mediated lipolysis via ATGL in adipocytes, I tested whether ATGL expressions are changed upon PKA activation. As shown in Figures 34A and B, treatment of forskolin, adenylyl cyclase activator, increased the level of ATGL protein. Instead, mRNA level of ATGL was not significantly changed, although there was a tendency to increase until 6-hour treatment of forskolin and then to decrease afterward (Fig 34C). Moreover, ATGL protein level was also increased by knockdown of PKA RIα and RIIβ, despite the decrease in mRNA levels (Fig. 34D, 32B). Consistent with the data from glycerol release and lipid droplet morphology, increased ATGL protein level was recovered by knockdown of PKA catalytic subunits (Fig. 34D). Therefore, it is likely that PKA activation could promote lipolysis via post-transcriptional regulation of ATGL.

PKA regulatory subunit IIβ expression is decreased in adipose tissue of obese

subjects

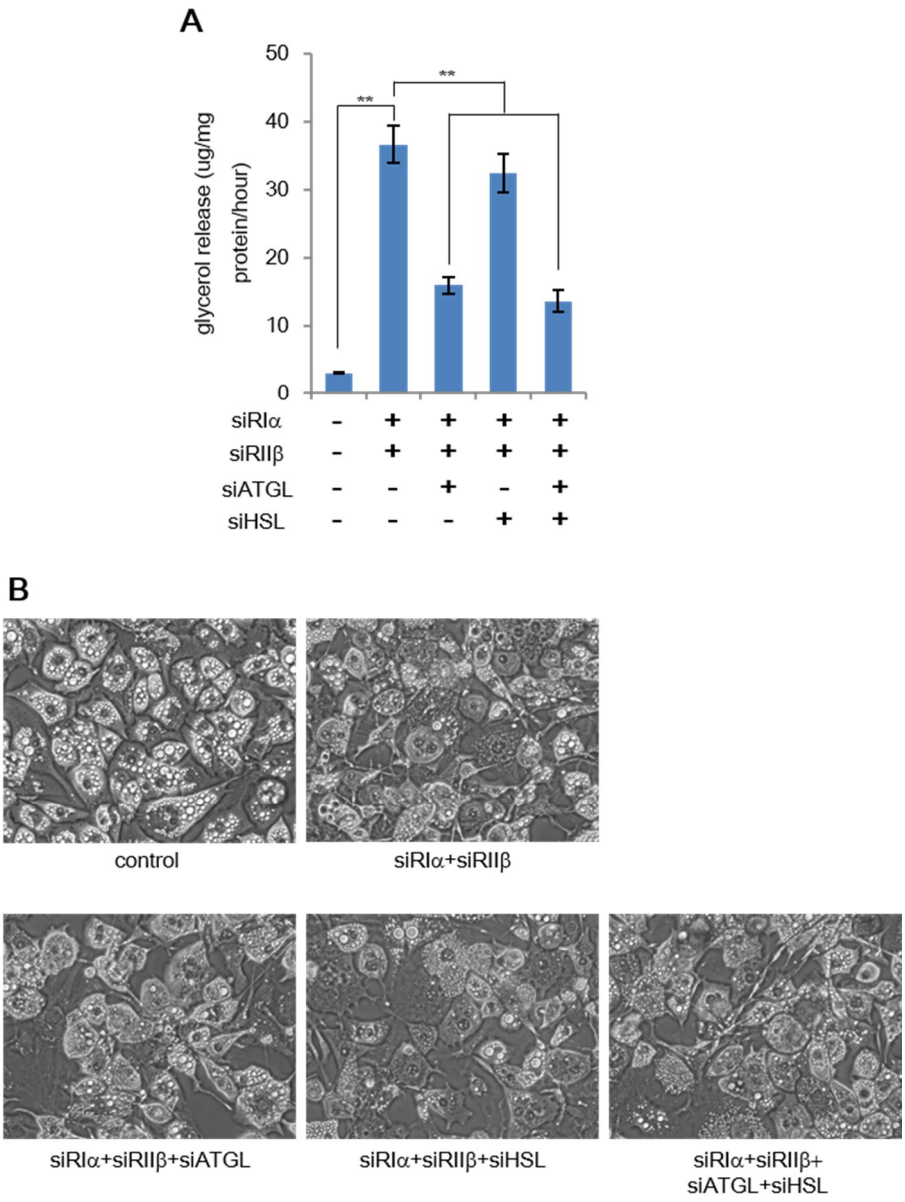

Figure 33. Effects of PKA regulatory subunit knockdown is partially suppressed by knockdown of ATGL.

(A) Glycerol concentrations of the media from fully differentiated 3T3-L1 adipocytes were measured 24 hours after siRNA transfection and normalized by total protein and time. (B) Phase contrast images of 3T3-L1 adipocytes 48 hours after siRNA transfection. Error bars represent standard deviations. **, $P < 0.01$.

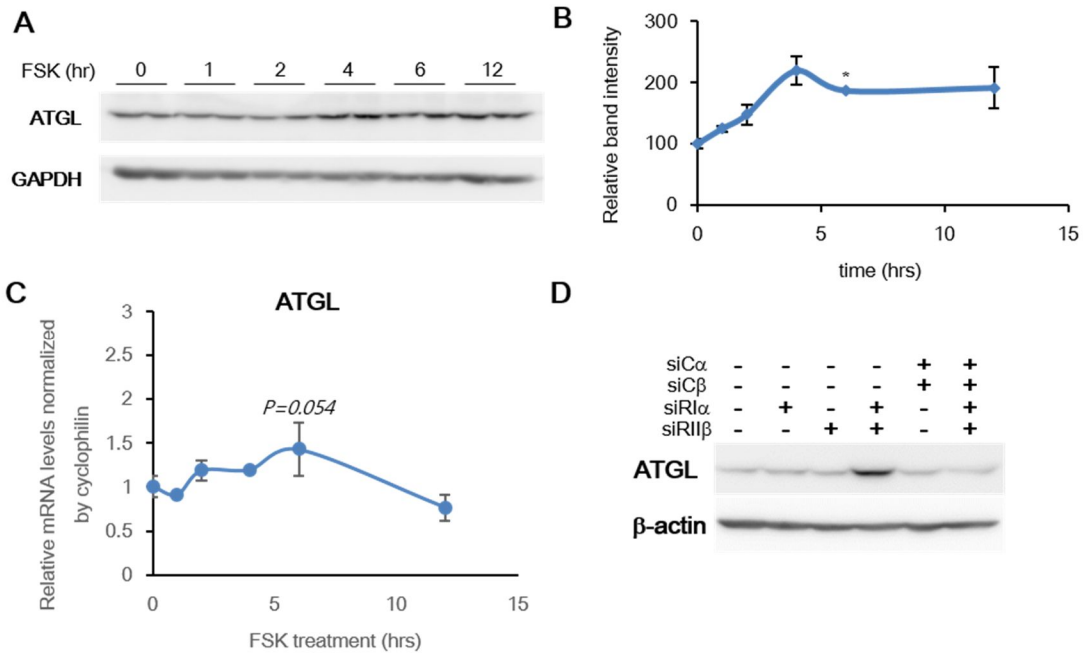

Figure 34. PKA activation increases ATGL expression in 3T3-L1 adipocytes.

(A and B) Western blot analysis and quantitation of mammalian ATGL protein levels in differentiated 3T3-L1 adipocytes treated with forskolin (FSK; 20 M) for the indicated time periods. The GAPDH protein was used as a loading control. (C) mRNA levels of ATGL measured by qRT-PCR and normalized to cyclophilin mRNA. (D) Western blot of mammalian ATGL protein in differentiated 3T3-L1 adipocytes 48 hours after siRNA transfection. The - actin protein was used as a loading control. Error bars represent standard deviations. *, $P < 0.05$ vs. time 0-h.

It has been shown that hyperlipidemia is often accompanied with obesity [113, 114]. To investigate potential role of PKA subunit imbalance in obesity, I analyzed mRNA expression levels of PKA subunits in diet-induced obesity model mice. In the adipose tissue of obese mice, RIIβ subunit expression was significantly down-regulated (Fig. 35). RIα subunit expression showed a slightly decreasing tendency and expressions of other subunits were not changed. These data suggest a potential role of PKA regulatory subunits in the increased basal lipolysis in obesity.

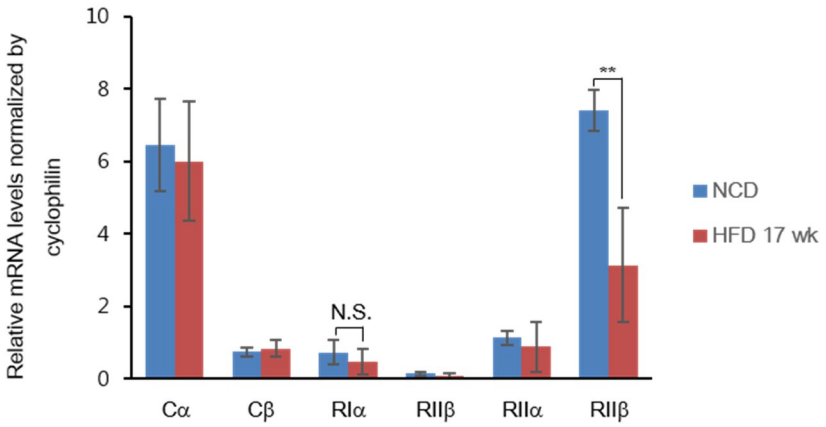

Figure 35. Expression of PKA RIIβ subunit is down-regulated in adipose tissue of HFD-fed mice.

(A) mRNA levels of PKA subunits were measured by qRT-PCR in the adipose tissue of control and high-fat diet fed mice. mRNA levels were normalized to cyclophilin mRNA. cyclophilin level was considered as 1. Error bars represent standard deviations. **, $P < 0.01$; N.S., not significant.

IV. Discussion

PKA signaling is a well-conserved pathway that regulates lipolysis. In fasted animals, hydrolysis of stored lipid metabolites is precisely regulated in a timely fashion via PKA to provide an energy source. Because excess lipid accumulation is often associated with metabolic dysregulation, lipase activity should be finely tuned in response to fasting signals. This study suggests that *C. elegans* would prevent unwanted lipolytic activity through proteasomal degradation of a key lipase ATGL-1, even without Perilipin 1 (Plin1) protein which plays a barrier function to inhibit lipolysis in mammals under basal conditions. I have demonstrated that in fasted worms, activated PKA would stabilize the ATGL-1 protein and drive ATGL-1 to localize on lipid droplets through interaction with the lipid droplet-binding protein LID-1, eventually leading to hydrolysis of stored lipid droplets in intestinal cells (Fig. 18). I also suggest that, in mammalian adipocytes, RIα and RIIβ subunits of PKA could play critical functions to keep the lipolytic activity low at basal state. In addition, it is likely that decreased expression of regulatory subunits could dramatically induce lipolysis in cell-autonomous manner, which might be one of the potential causes of hyperlipidemia in obesity.

IV-1. LID-1/ATGL-1 mediated lipolysis upon fasting in *C. elegans*

In *C. elegans*, *atgl-1* plays crucial role in fasting-induced lipolysis. Besides *atgl-1*, RNAi of *lips-1, lips-2, lips-13, fil-1, D1054.1,* and *C03E3.9* also partially attenuated fasting-induced lipid hydrolysis (Fig. 2A). Thus, *C. elegans* may use several lipases to accommodate various nutritional changes. However, our data evidently show that knockdown of *atgl-1* or *lid-1* impedes fasting-induced lipolysis in adult worms. It has been well established that ATGL is essential for lipolysis in mammalian adipocytes and that ATGL-deficient mice show systemic lipid accumulation [22, 24]. In addition, CGI-58, a homolog of *lid-1*, has been identified as a

causative gene of Chanarin-Dorfman syndrome, a rare recessive genetic disease with systemic lipid accumulation and ichthyosis [28, 115]. Thus, my data indicate that *atgl-1* and *lid-1* are functionally well conserved throughout the evolution to execute and coordinate lipolytic metabolism.

Lipid droplets are dynamic cellular organelles coated with various proteins, and there are significant similarities in lipid droplet proteins between mammals and *C. elegans* [1, 106, 116]. On the other hand, as perilipin family of lipid droplet proteins is well conserved from *Dictyostelium* to humans, lack of the perilipin-domain containing gene in *C. elegans* seems to place LID-1 at a unique position in the evolution of lipolytic machinery (Fig. 4). In this study, I propose that LID-1 may be an ortholog of mammalian CGI-58. Nevertheless, it seems that LID-1 would possess distinct features from CGI-58 in following aspects. First, LID-1 is constitutively localized at lipid droplets (Fig. 6). Second, unlike mammalian CGI-58, LID-1 does not require perilipin proteins to target on lipid droplets, although LID-1 may not fulfill the role of Plin1 in *C. elegans*. For instance, unlike Plin1, LID-1 does not have anti-lipolytic function since suppression of *lid-1* slightly increased fat contents in worms (Fig. 7), whereas ablation of Plin1 greatly promotes the basal lipolytic activity in mammalian adipocytes [9, 117]. Given that mammalian CGI-58 requires Plin1 to localize to lipid droplets [29], it needs to be determined whether LID-1 can localize to lipid droplets by itself without other proteins. During evolution, it appears that perilipin family proteins might be emerged with the needs of constituting large lipid droplets in specialized fat-storing cells with greater capability for energy source storage. Thus, it is likely that *C. elegans*, which lacks perilipin, may have evolved its own regulatory mechanisms using protein stability to control lipase activity upon LID-1 accessibility, which may be distinct from mammals.

Several regulatory mechanisms for lipases have evolved with different lipid droplet

proteins. For example, in yeast, which lacks both CGI-58 and perilipin, triglyceride hydrolase TGL4 is constitutively localized on the surface of lipid droplets and its activity is regulated by the cyclin-dependent kinase Cdc28 [118]. In fly, expression of Brummer lipase is increased by starvation, leading to increase in lipolytic activity [119]. In mammals, HSL is well known to be regulated by its translocation to lipid droplets with Plin1 [8, 13]. Furthermore, mammalian ATGL transcription is upregulated in response to fasting [21, 26, 120], and ATGL activity is promoted by binding to CGI-58, which is released from Plin1 upon PKA activation [32, 121]. In *C. elegans*, I would like to suggest that proteasomal degradation of ATGL-1 prevents futile lipolysis during feeding, and PKA-dependent phosphorylation and stabilization of ATGL-1 protein stimulates LID-1 binding and lipase activity during fasting. Similar to *C. elegans* ATGL-1, I observed that the mammalian ATGL protein was increased by PKA activation in adipocytes. Furthermore, it has been recently reported that mammalian ATGL protein is regulated by proteasomal degradation [122, 123], indicating the possibility of an evolutionarily conserved mechanism. Interestingly, very recent study showed that serotonin and octopamine signaling promotes body fat loss via transcriptional upregulation of ATGL-1, suggesting an additional layer of regulatory mechanism of lipolysis [124]. In regard to spatial and temporal regulation of lipase(s), it is plausible to speculate that regulation of protein stability and translocation of certain lipase(s) would be an efficient way to activate lipolysis, assuring immediate response to fasting. Of course, I cannot exclude the possibility that phosphorylation of ATGL-1 may affect its own hydrolase activity.

Previously, it has been reported that AMPK also phosphorylates *atgl-1* at multiple sites and downregulates hydrolase activity to ration lipid reserves during long-term starvation at the dauer stage [84]. Consistently, I also observed that AMPK might attenuate lipolysis in fasted adult worms, implying that PKA and AMPK may regulate *atgl-1* in opposite ways with different repertoires of phosphorylation and molecular components. It appears that PKA is rapidly

activated at the initial phase of fasting. Immediate activation of lipid hydrolysis by PKA upon fasting would not be sustainable for long-term starvation. In addition, I observed that cAMP levels returned to basal levels after 8 hours of fasting. On the contrary, it is likely that AMPK would restrain excessive lipolysis during fasting to prevent energy depletion. As previously suggested, it is possible that *C. elegans* may exhibit bi-phasic metabolic responses in nutrient deprivations: rapid consumption of stored lipid metabolites with high metabolic activity followed by inert preservation mode with low metabolic activity [125]. Furthermore, it has been demonstrated that in mammalian cells, AMPK is activated as a consequence of lipolysis and inhibits further lipolysis forming a negative feedback control [126, 127]. Together, a recent study showed that hydrolase activity of mouse ATGL is enhanced via phosphorylation by PKA [33], suggesting that ATGL would be a conserved target of PKA. Further studies are required to address the crosstalk between PKA and AMPK signaling in the control of lipolysis at various developmental stages of *C. elegans* under different nutritional conditions.

In this study, I identified a lipid droplet protein LID-1 and examined its subcellular colocalization with certain lipophilic dyes. The nature of lipid droplets in *C. elegans* has been controversial due to heterogeneity of staining granules in intestinal cells [98]. Localizations of GFP-fused LID-1 protein and lipid-staining dyes showed different patterns depending on the staining methods. For instance, LID-1 colocalized with Oil Red O-positive lipid droplets after fixative staining. However, LID-1 did not colocalize with the Nile Red dye without fixation in live worms, whereas LID-1 colocalized with Nile Red-positive granules after fixation. These results suggest that, in the live state, certain biological processes in the intestinal cells of *C. elegans* may exclude Nile Red from LID-1-positive lipid droplets. Despite these methodological discrepancies, GFP-fused LID-1, which was constitutively localized on lipid droplets, can be used for the visualization of lipid droplets in both live and fixed worms.

IV-2. Genetic screening for the mediator of PKA-induced lipolysis in *C. elegans*

In addition to its powerful genetics, *C. elegans* provides an excellent model for studying PKA pathway in vivo. Unlike mammals, *C. elegans* has only single genes for each PKA catalytic and regulatory subunit, and PKA activity can be easily modulated by knockdown. Knockdown of *kin-2* gene, which encodes a regulatory subunit of PKA, leads to pleiotropic phenotypes. Upon kin-2 RNAi, worms showed dumpy morphology, decreased Nile Red-stained granules, defects in locomotion, sterility as well as decreased Oil-Red O stained lipid droplets. These suggest that PKA in *C. elegans* may be involved in variety of processes including formation of cuticle exoskeleton, neuromuscular functions, reproduction, and maintenance of lysosome-related organelles and lipid droplets. Through the random mutagenesis screening using *C. elegans*, I have isolated three mutants that could rescue *kin-2* RNAi phenotypes. As candidate gene lists of each mutant have been obtained by SNP mapping and whole-genome sequencing, the next step would be to verify genes as true *kin-2* suppressors by analyzing available mutants or RNAi phenotypes. For efficiency, candidate genes will be given priorities according to the predicted severity of mutations.

Although the screening process is still incomplete, my data suggest important clues on the function of PKA pathway in *C. elegans*. First, this screening was not a saturated mutagenesis screening using ~18,000 F1 haploid genotypes. However, three viable mutants I have isolated have different mutations as chromosome mapping results indicate. Therefore, it is highly possible that there would be more *kin-2* suppressor genes which have not been isolated by this screening. Second, all three mutants rescued sterility, dumpy morphology, and decreased Nile Red staining phenotypes of *kin-2* RNAi. I failed to isolate viable mutants that specifically rescue Nile Red staining which would reflect lipid storage in lysosome-related organelles. This

result suggests that different phenotypes of *kin-2* RNAi are linked to one another and isolated mutants might be involved in general PKA activity modulation rather than the genes being involved with some specific function of PKA. Lastly, most mutants that rescue selective *kin-2* RNAi phenotype might be excluded because of viability or sterility. Given that PKA signaling plays important roles in growth, development, and reproduction, certain mutations that suppress PKA function might not be recovered in this screening procedure due to the severe defects.

IV-3. PKA regulatory subunits and lipolysis in mammalian adipocytes

In mammalian adipocytes, RIIβ is the predominant regulatory subunit that composes PKA. The core function of regulatory subunits is to repress catalytic subunits in the absence of cAMP. In this study, using combinatorial suppression of PKA subunits with siRNA, I have demonstrated that RIα and RIIβ subunits of PKA are required for maintenance of lipolytic suppression and lipid droplet formation in basal state of adipocytes. Loss of RIα and RIIβ subunits are sufficient to induce lipolysis and to decrease lipid droplets without any exogenous lipolytic stimulation. And these phenotypes were fully dependent on catalytic subunits of PKA and dependent on ATGL.

As in *C. elegans*, PKA pathway in mammalian adipocytes also requires ATGL for activation of lipolysis. Previously, it has been reported that ATGL is known to be mainly regulated at transcript level. ATGL mRNA expression is increased by fasting and glucocorticoid and decreased by refeeding and insulin [21, 27]. However, current data showed that ATGL protein level was not always correlated with ATGL mRNA level. The finding that ATGL protein is increased by PKA activation provides an additional layer of regulatory mechanisms of ATGL. It is of interest to note that both *C. elegans* and mammals utilize similar process, PKA induced up-regulation of ATGL protein level. These results indicate evolutionarily conserved function of

this pathway. Also, recent report showed that mammalian ATGL is phosphorylated and activated by PKA [33]. However, further studies are necessary to unravel how PKA activation increases ATGL protein levels in mammalian adipocytes.

Gene expression analysis showed that mRNA levels of genes involved in lipid metabolism were largely altered by suppression of PKA regulatory subunits with siRNA. Given that perilipin null adipocytes have increased basal lipolysis, decreased expression of perilipin could be one of possible mechanisms of PKA regulatory subunit suppression phenotypes. In addition, increased CGI-58 expression could lead to activation of ATGL. Nevertheless, as PKA signaling is associated with various cellular processes, gene expression might be indirectly affected by PKA system alteration.

PKA subunits in mammals exhibit different tissue distribution and biochemical properties. In adipose tissue, RIIβ subunit has been reported to be a major regulatory subunit of PKA. For example, it has been shown that RIIβ subunit-deficient mice exhibit lean and are resistant to diet-induced obesity [64, 65, 67, 128]. In the adipose tissue of RIIβ knockout mice, RIα subunit expression shows a compensatory increase, which leads to increased cAMP sensitivity and basal lipolysis. However, my data and another report indicate that, in obesity, the expression of RIIβ is decreased without the compensatory effect of other regulatory subunits in the adipose tissue [129]. Thus, it is possible that genetic deletion of RIIβ would cause RIα induction, which may not be accompanied in the development of obesity. Given that dysregulation of lipolysis is observed in obesity, it is plausible to speculate that the decrease of RIIβ subunits without compensatory increase of other regulatory subunits, especially RIα, might be the potential cause of increased basal lipolysis.

However, it is still unclear whether decreased expression of PKA RIIβ subunit may be a major factor of increased basal lipolysis in obese adipose tissue. It needs to be investigated

whether RIα subunit is not compensating for the decreased RIIβ subunit. Further, it appears that large lipid droplets of hypertrophied adipocytes observed in adipose tissues of obese subjects are different from those of adipocytes with regulatory subunit knockdown. In addition, although my data indicate that ATGL protein up-regulation would be one of is potential causes of increased lipolysis upon regulatory subunit deficiency, it has been reported that ATGL mRNA is down-regulated in genetically obese mice (*ob/ob* and *db/db* mice) [21, 25]. Also, there are controversies in human adipose tissue studies. For instance, it has been reported that both ATGL mRNA and protein levels are decreased in obese individuals [130, 131]. However, other report suggest ATGL mRNA and protein levels in adipose tissue are not affected by obesity and weight reduction [132], indicating the complexity of ATGL expression regulation and/or individual differences of human patients. Therefore, further studies are required to examine PKA activity in correlation with ATGL protein expressions in the adipose tissue. In addition, questions still remain on which factors are involved in the expression of PKA subunits and how early PKA subunit alteration occurs upon obesity. Also, I cannot exclude the possibility that imbalance in expression of PKA subunit might be involved in other diseases accompanied with dysregulation of lipid metabolism. For instance, increased lipolysis and reduced lipid droplet in adipocytes are hallmarks of lipodystrophy[133, 134] and cachexia [135-137], suggesting a potential involvement of PKA subunit dysregulation in these diseases.

V. Conclusion and perspectives

In conclusion, I have identified the regulatory mechanisms of PKA-mediated lipolysis in *C. elegans* and mammalian adipocytes. For tight control of lipolysis, both suppression of unwanted lipolysis at basal state and activation of lipolysis at fasting state are important. In the absence of perilipin acting as a barrier against lipolysis, *C. elegans* suppresses unnecessary lipolysis by actively degrading ATGL-1 protein. Upon nutritional depletion, *C. elegans* activates PKA signaling to stabilize ATGL-1, which could induce its association with the lipid droplet protein LID-1 to activate the lipase function of ATGL-1, resulting in energy production. For efficient and immediate responses to fasting in *C. elegans,* stabilized ATGL-1 forms a protein complex with LID-1 at lipid droplets, ensuring prompt lipolytic activity. My data highlights the cooperative action of LID-1 for proper functions of the lipase ATGL-1 to maintain energy homeostasis following nutritional changes. However, several questions remain to be answered in order to understand energy metabolism of *C. elegans* under fasting. For example, how does *C. elegans* sense fasting signal? Is fasting-induced lipolysis required for survival of worms under fasting? Do worms utilize stored lipids during fasting for what? Energy consuming processes such as locomotion or reproduction would need energy by burning stored lipids during food deprivation. As most organisms do, *C. elegans* might have stored energy sources other than lipids, such as glycogen. Despite of many questions raised above, it is likely that *C. elegans* provides an excellent genetic model organism for studying lipid metabolism regulation upon various stress conditions, which may potentially implicate in dysregulation of lipid metabolism in human diseases

In mammalian adipocytes, I have characterized functional specificity of PKA subunits in the regulation of lipolysis. It appears that PKA and lipolysis are highly inducible systems in adipocytes. Basal PKA activity is tightly controlled by regulatory subunits and PKA is acutely

activated by fasting or hormonal signals for the energy homeostasis without lipotoxicity. Functional roles of PKA RIα and RIIβ regulatory subunits are critical for the maintenance of basal lipid homeostasis and lipid droplet formation. Decrease in the expressions of PKA regulatory subunits can lead to increased lipolytic activity via ATGL without stimulatory hormones. Interestingly, I have observed that ATGL protein level is increased by PKA activation. It seems that the control of lipase at protein level is a well-conserved process in both *C. elegans* and mammals. Collectively, these results suggest the importance of both basal and stimulated PKA signaling in lipase activity control and disruption in PKA system might be a potential cause for diseases with lipid dysregulation.

VI. References

1. Martin, S. and R.G. Parton, *Lipid droplets: a unified view of a dynamic organelle.* Nat Rev Mol Cell Biol, 2006. **7**(5): p. 373-8.
2. Cermelli, S., et al., *The lipid-droplet proteome reveals that droplets are a protein-storage depot.* Curr Biol, 2006. **16**(18): p. 1783-95.
3. Brasaemle, D.L., et al., *Proteomic analysis of proteins associated with lipid droplets of basal and lipolytically stimulated 3T3-L1 adipocytes.* J Biol Chem, 2004. **279**(45): p. 46835-42.
4. Miura, S., et al., *Functional conservation for lipid storage droplet association among Perilipin, ADRP, and TIP47 (PAT)-related proteins in mammals, Drosophila, and Dictyostelium.* J Biol Chem, 2002. **277**(35): p. 32253-7.
5. Brasaemle, D.L., *Thematic review series: adipocyte biology. The perilipin family of structural lipid droplet proteins: stabilization of lipid droplets and control of lipolysis.* J Lipid Res, 2007. **48**(12): p. 2547-59.
6. Bickel, P.E., J.T. Tansey, and M.A. Welte, *PAT proteins, an ancient family of lipid droplet proteins that regulate cellular lipid stores.* Biochim Biophys Acta, 2009. **1791**(6): p. 419-40.
7. Sztalryd, C. and A.R. Kimmel, *Perilipins: lipid droplet coat proteins adapted for tissue-specific energy storage and utilization, and lipid cytoprotection.* Biochimie, 2014. **96**: p. 96-101.
8. Sztalryd, C., et al., *Perilipin A is essential for the translocation of hormone-sensitive lipase during lipolytic activation.* J Cell Biol, 2003. **161**(6): p. 1093-103.
9. Tansey, J.T., et al., *Perilipin ablation results in a lean mouse with aberrant adipocyte lipolysis, enhanced leptin production, and resistance to diet-induced obesity.* Proc Natl Acad Sci U S A, 2001. **98**(11): p. 6494-9.
10. Carmen, G.Y. and S.M. Victor, *Signalling mechanisms regulating lipolysis.* Cell Signal, 2006. **18**(4): p. 401-8.
11. Unger, R.H., et al., *Lipid homeostasis, lipotoxicity and the metabolic syndrome.* Biochim Biophys Acta, 2010. **1801**(3): p. 209-14.
12. Holm, C., *Molecular mechanisms regulating hormone-sensitive lipase and lipolysis.* Biochem Soc Trans, 2003. **31**(Pt 6): p. 1120-4.
13. Egan, J.J., et al., *Mechanism of hormone-stimulated lipolysis in adipocytes: translocation of hormone-sensitive lipase to the lipid storage droplet.* Proc Natl Acad Sci U S A, 1992. **89**(18): p. 8537-41.
14. Stralfors, P., P. Bjorgell, and P. Belfrage, *Hormonal regulation of hormone-sensitive*

lipase in intact adipocytes: identification of phosphorylated sites and effects on the phosphorylation by lipolytic hormones and insulin. Proc Natl Acad Sci U S A, 1984. **81**(11): p. 3317-21.

15. Anthonsen, M.W., et al., *Identification of novel phosphorylation sites in hormone-sensitive lipase that are phosphorylated in response to isoproterenol and govern activation properties in vitro.* J Biol Chem, 1998. **273**(1): p. 215-21.
16. Zhang, H.H., et al., *Lipase-selective functional domains of perilipin A differentially regulate constitutive and protein kinase A-stimulated lipolysis.* J Biol Chem, 2003. **278**(51): p. 51535-42.
17. Jenkins-Kruchten, A.E., et al., *Fatty acid-binding protein-hormone-sensitive lipase interaction. Fatty acid dependence on binding.* J Biol Chem, 2003. **278**(48): p. 47636-43.
18. Osuga, J., et al., *Targeted disruption of hormone-sensitive lipase results in male sterility and adipocyte hypertrophy, but not in obesity.* Proc Natl Acad Sci U S A, 2000. **97**(2): p. 787-92.
19. Haemmerle, G., et al., *Hormone-sensitive lipase deficiency in mice causes diglyceride accumulation in adipose tissue, muscle, and testis.* J Biol Chem, 2002. **277**(7): p. 4806-15.
20. Wang, S.P., et al., *The adipose tissue phenotype of hormone-sensitive lipase deficiency in mice.* Obes Res, 2001. **9**(2): p. 119-28.
21. Villena, J.A., et al., *Desnutrin, an adipocyte gene encoding a novel patatin domain-containing protein, is induced by fasting and glucocorticoids: ectopic expression of desnutrin increases triglyceride hydrolysis.* J Biol Chem, 2004. **279**(45): p. 47066-75.
22. Zimmermann, R., et al., *Fat mobilization in adipose tissue is promoted by adipose triglyceride lipase.* Science, 2004. **306**(5700): p. 1383-6.
23. Jenkins, C.M., et al., *Identification, cloning, expression, and purification of three novel human calcium-independent phospholipase A2 family members possessing triacylglycerol lipase and acylglycerol transacylase activities.* J Biol Chem, 2004. **279**(47): p. 48968-75.
24. Haemmerle, G., et al., *Defective lipolysis and altered energy metabolism in mice lacking adipose triglyceride lipase.* Science, 2006. **312**(5774): p. 734-7.
25. Kim, J.Y., et al., *The adipose tissue triglyceride lipase ATGL/PNPLA2 is downregulated by insulin and TNF-alpha in 3T3-L1 adipocytes and is a target for transactivation by PPARgamma.* Am J Physiol Endocrinol Metab, 2006. **291**(1): p. E115-27.
26. Kershaw, E.E., et al., *Adipose triglyceride lipase: function, regulation by insulin, and comparison with adiponutrin.* Diabetes, 2006. **55**(1): p. 148-57.

27. Kralisch, S., et al., *Isoproterenol, TNFalpha, and insulin downregulate adipose triglyceride lipase in 3T3-L1 adipocytes.* Mol Cell Endocrinol, 2005. **240**(1-2): p. 43-9.
28. Lass, A., et al., *Adipose triglyceride lipase-mediated lipolysis of cellular fat stores is activated by CGI-58 and defective in Chanarin-Dorfman Syndrome.* Cell Metab, 2006. **3**(5): p. 309-19.
29. Subramanian, V., et al., *Perilipin A mediates the reversible binding of CGI-58 to lipid droplets in 3T3-L1 adipocytes.* J Biol Chem, 2004. **279**(40): p. 42062-71.
30. Yamaguchi, T., et al., *CGI-58 interacts with perilipin and is localized to lipid droplets. Possible involvement of CGI-58 mislocalization in Chanarin-Dorfman syndrome.* J Biol Chem, 2004. **279**(29): p. 30490-7.
31. Granneman, J.G., et al., *Analysis of lipolytic protein trafficking and interactions in adipocytes.* J Biol Chem, 2007. **282**(8): p. 5726-35.
32. Granneman, J.G., et al., *Perilipin controls lipolysis by regulating the interactions of AB-hydrolase containing 5 (Abhd5) and adipose triglyceride lipase (Atgl).* J Biol Chem, 2009. **284**(50): p. 34538-44.
33. Pagnon, J., et al., *Identification and functional characterization of protein kinase A phosphorylation sites in the major lipolytic protein, adipose triglyceride lipase.* Endocrinology, 2012. **153**(9): p. 4278-89.
34. Wijkander, J., et al., *Insulin-induced phosphorylation and activation of phosphodiesterase 3B in rat adipocytes: possible role for protein kinase B but not mitogen-activated protein kinase or p70 S6 kinase.* Endocrinology, 1998. **139**(1): p. 219-27.
35. Duncan, R.E., et al., *Regulation of lipolysis in adipocytes.* Annu Rev Nutr, 2007. **27**: p. 79-101.
36. Zmuda-Trzebiatowska, E., et al., *Role of PDE3B in insulin-induced glucose uptake, GLUT-4 translocation and lipogenesis in primary rat adipocytes.* Cell Signal, 2006. **18**(3): p. 382-90.
37. Arner, P., *Human fat cell lipolysis: biochemistry, regulation and clinical role.* Best Pract Res Clin Endocrinol Metab, 2005. **19**(4): p. 471-82.
38. Taggart, A.K., et al., *(D)-beta-Hydroxybutyrate inhibits adipocyte lipolysis via the nicotinic acid receptor PUMA-G.* J Biol Chem, 2005. **280**(29): p. 26649-52.
39. Ryden, M., et al., *Targets for TNF-alpha-induced lipolysis in human adipocytes.* Biochem Biophys Res Commun, 2004. **318**(1): p. 168-75.
40. Ryden, M., et al., *Mapping of early signaling events in tumor necrosis factor-alpha -mediated lipolysis in human fat cells.* J Biol Chem, 2002. **277**(2): p. 1085-91.
41. Berthet, J., E.W. Sutherland, and T.W. Rall, *The assay of glucagon and epinephrine*

with use of liver homogenates. J Biol Chem, 1957. **229**(1): p. 351-61.

42. Rall, T.W. and E.W. Sutherland, *Formation of a cyclic adenine ribonucleotide by tissue particles.* J Biol Chem, 1958. **232**(2): p. 1065-76.
43. Sutherland, E.W. and T.W. Rall, *Fractionation and characterization of a cyclic adenine ribonucleotide formed by tissue particles.* J Biol Chem, 1958. **232**(2): p. 1077-91.
44. Krebs, E.G., D.J. Graves, and E.H. Fischer, *Factors affecting the activity of muscle phosphorylase b kinase.* J Biol Chem, 1959. **234**: p. 2867-73.
45. Granot, J., et al., *Magnetic resonance studies of the effect of the regulatory subunit on metal and substrate binding to the catalytic subunit of bovine heart protein kinase.* J Biol Chem, 1980. **255**(10): p. 4569-73.
46. Granot, J., A.S. Mildvan, and E.T. Kaiser, *Studies of the mechanism of action and regulation of cAMP-dependent protein kinase.* Arch Biochem Biophys, 1980. **205**(1): p. 1-17.
47. Kim, C., et al., *PKA-I holoenzyme structure reveals a mechanism for cAMP-dependent activation.* Cell, 2007. **130**(6): p. 1032-43.
48. Kim, C., N.H. Xuong, and S.S. Taylor, *Crystal structure of a complex between the catalytic and regulatory (RIalpha) subunits of PKA.* Science, 2005. **307**(5710): p. 690-6.
49. McKnight, G.S., *Cyclic AMP second messenger systems.* Curr Opin Cell Biol, 1991. **3**(2): p. 213-7.
50. Corbin, J.D., S.L. Keely, and C.R. Park, *The distribution and dissociation of cyclic adenosine 3':5'-monophosphate-dependent protein kinases in adipose, cardiac, and other tissues.* J Biol Chem, 1975. **250**(1): p. 218-25.
51. Doskeland, S.O. and P.M. Ueland, *Binding proteins for adenosine 3':5'-cyclic monophosphate in bovine adrenal cortex.* Biochem J, 1977. **165**(3): p. 561-73.
52. Schwechheimer, K. and F. Hofmann, *Properties of regulatory subunit of cyclic AMP-dependent protein kinase (peak I) from rabbit skeletal muscle prepared by urea treatment of the holoenzyme.* J Biol Chem, 1977. **252**(21): p. 7690-6.
53. Buss, J.E., R.W. McCune, and G.N. Gill, *Comparison of cyclic nucleotide binding to adenosine 3',5'-monophosphate and guanosine 3',5'-monophosphate-dependent protein kinases.* J Cyclic Nucleotide Res, 1979. **5**(3): p. 225-37.
54. Sanborn, B.M. and S.G. Korenman, *Further studies of the interaction of cyclic adenosine 3':5'-monophosphate with endometrial protein kinase.* J Biol Chem, 1973. **248**(13): p. 4713-5.
55. Hofmann, F., *Apparent constants for the interaction of regulatory and catalytic subunit of cAMP-dependent protein kinase Ⅰ and Ⅱ.* J Biol Chem, 1980. **255**(4): p. 1559-64.

56. Shabb, J.B., *Physiological substrates of cAMP-dependent protein kinase.* Chem Rev, 2001. **101**(8): p. 2381-411.
57. Gao, X., et al., *Proteome-wide prediction of PKA phosphorylation sites in eukaryotic kingdom.* Genomics, 2008. **92**(6): p. 457-63.
58. Amieux, P.S., et al., *Increased basal cAMP-dependent protein kinase activity inhibits the formation of mesoderm-derived structures in the developing mouse embryo.* J Biol Chem, 2002. **277**(30): p. 27294-304.
59. Kirschner, L.S., et al., *A mouse model for the Carney complex tumor syndrome develops neoplasia in cyclic AMP-responsive tissues.* Cancer Res, 2005. **65**(11): p. 4506-14.
60. Skalhegg, B.S., et al., *Mutation of the Calpha subunit of PKA leads to growth retardation and sperm dysfunction.* Mol Endocrinol, 2002. **16**(3): p. 630-9.
61. Howe, D.G., J.C. Wiley, and G.S. McKnight, *Molecular and behavioral effects of a null mutation in all PKA C beta isoforms.* Mol Cell Neurosci, 2002. **20**(3): p. 515-24.
62. Brandon, E.P., et al., *Hippocampal long-term depression and depotentiation are defective in mice carrying a targeted disruption of the gene encoding the RI beta subunit of cAMP-dependent protein kinase.* Proc Natl Acad Sci U S A, 1995. **92**(19): p. 8851-5.
63. Burton, K.A., et al., *Type II regulatory subunits are not required for the anchoring-dependent modulation of Ca2+ channel activity by cAMP-dependent protein kinase.* Proc Natl Acad Sci U S A, 1997. **94**(20): p. 11067-72.
64. Cummings, D.E., et al., *Genetically lean mice result from targeted disruption of the RII beta subunit of protein kinase A.* Nature, 1996. **382**(6592): p. 622-6.
65. Schreyer, S.A., et al., *Mutation of the RIIbeta subunit of protein kinase A prevents diet-induced insulin resistance and dyslipidemia in mice.* Diabetes, 2001. **50**(11): p. 2555-62.
66. Amieux, P.S., et al., *Compensatory regulation of RIalpha protein levels in protein kinase A mutant mice.* J Biol Chem, 1997. **272**(7): p. 3993-8.
67. Planas, J.V., et al., *Mutation of the RIIbeta subunit of protein kinase A differentially affects lipolysis but not gene induction in white adipose tissue.* J Biol Chem, 1999. **274**(51): p. 36281-7.
68. Ashrafi, K., et al., *Genome-wide RNAi analysis of Caenorhabditis elegans fat regulatory genes.* Nature, 2003. **421**(6920): p. 268-72.
69. Jones, K.T. and K. Ashrafi, *Caenorhabditis elegans as an emerging model for studying the basic biology of obesity.* Dis Model Mech, 2009. **2**(5-6): p. 224-9.
70. Johnson, T.E., et al., *Arresting development arrests aging in the nematode*

Caenorhabditis elegans. Mech Ageing Dev, 1984. **28**(1): p. 23-40.

71. Cassada, R.C. and R.L. Russell, *The dauerlarva, a post-embryonic developmental variant of the nematode Caenorhabditis elegans.* Dev Biol, 1975. **46**(2): p. 326-42.
72. Golden, J.W. and D.L. Riddle, *The Caenorhabditis elegans dauer larva: developmental effects of pheromone, food, and temperature.* Dev Biol, 1984. **102**(2): p. 368-78.
73. Van Gilst, M.R., H. Hadjivassiliou, and K.R. Yamamoto, *A Caenorhabditis elegans nutrient response system partially dependent on nuclear receptor NHR-49.* Proc Natl Acad Sci U S A, 2005. **102**(38): p. 13496-501.
74. Sawin, E.R., R. Ranganathan, and H.R. Horvitz, *C. elegans locomotory rate is modulated by the environment through a dopaminergic pathway and by experience through a serotonergic pathway.* Neuron, 2000. **26**(3): p. 619-31.
75. Avery, L. and H.R. Horvitz, *Effects of starvation and neuroactive drugs on feeding in Caenorhabditis elegans.* J Exp Zool, 1990. **253**(3): p. 263-70.
76. Angelo, G. and M.R. Van Gilst, *Starvation protects germline stem cells and extends reproductive longevity in C. elegans.* Science, 2009. **326**(5955): p. 954-8.
77. Trent, C., *Genetic and Behavioral Studies of the Egg-Laying System of Caenorhabditis elegans.* PhD Thesis, Massachusetts Institute of Technology, Cambridge, USA. , 1982.
78. Horvitz, H.R., et al., *Serotonin and octopamine in the nematode Caenorhabditis elegans.* Science, 1982. **216**(4549): p. 1012-4.
79. McKay, R.M., et al., *C elegans: a model for exploring the genetics of fat storage.* Dev Cell, 2003. **4**(1): p. 131-42.
80. Apfeld, J., et al., *The AMP-activated protein kinase AAK-2 links energy levels and insulin-like signals to lifespan in C. elegans.* Genes Dev, 2004. **18**(24): p. 3004-9.
81. Yang, F., et al., *An ARC/Mediator subunit required for SREBP control of cholesterol and lipid homeostasis.* Nature, 2006. **442**(7103): p. 700-4.
82. Jia, K., D. Chen, and D.L. Riddle, *The TOR pathway interacts with the insulin signaling pathway to regulate C. elegans larval development, metabolism and life span.* Development, 2004. **131**(16): p. 3897-906.
83. Gross, R.E., et al., *Cloning, characterization, and expression of the gene for the catalytic subunit of cAMP-dependent protein kinase in Caenorhabditis elegans. Identification of highly conserved and unique isoforms generated by alternative splicing.* J Biol Chem, 1990. **265**(12): p. 6896-907.
84. Narbonne, P. and R. Roy, *Caenorhabditis elegans dauers need LKB1/AMPK to ration lipid reserves and ensure long-term survival.* Nature, 2009. **457**(7226): p. 210-4.
85. Wang, M.C., E.J. O'Rourke, and G. Ruvkun, *Fat metabolism links germline stem cells and longevity in C. elegans.* Science, 2008. **322**(5903): p. 957-60.

86. O'Rourke, E.J., et al., *ω-6 Polyunsaturated fatty acids extend life span through the activation of autophagy.* Genes Dev, 2013. **27**(4): p. 429-40.
87. O'Rourke, E.J. and G. Ruvkun, *MXL-3 and HLH-30 transcriptionally link lipolysis and autophagy to nutrient availability.* Nat Cell Biol, 2013. **15**(6): p. 668-76.
88. Watts, J.L. and J. Browse, *Genetic dissection of polyunsaturated fatty acid synthesis in Caenorhabditis elegans.* Proc Natl Acad Sci U S A, 2002. **99**(9): p. 5854-9.
89. Watts, J.L. and J. Browse, *A palmitoyl-CoA-specific delta9 fatty acid desaturase from Caenorhabditis elegans.* Biochem Biophys Res Commun, 2000. **272**(1): p. 263-9.
90. Brock, T.J., J. Browse, and J.L. Watts, *Fatty acid desaturation and the regulation of adiposity in Caenorhabditis elegans.* Genetics, 2007. **176**(2): p. 865-75.
91. Watts, J.L., *Fat synthesis and adiposity regulation in Caenorhabditis elegans.* Trends Endocrinol Metab, 2009. **20**(2): p. 58-65.
92. Kniazeva, M., et al., *Monomethyl branched-chain fatty acids play an essential role in Caenorhabditis elegans development.* PLoS Biol, 2004. **2**(9): p. E257.
93. Kniazeva, M., T. Euler, and M. Han, *A branched-chain fatty acid is involved in post-embryonic growth control in parallel to the insulin receptor pathway and its biosynthesis is feedback-regulated in C. elegans.* Genes Dev, 2008. **22**(15): p. 2102-10.
94. Hermann, G.J., et al., *Genetic analysis of lysosomal trafficking in Caenorhabditis elegans.* Mol Biol Cell, 2005. **16**(7): p. 3273-88.
95. Schroeder, L.K., et al., *Function of the Caenorhabditis elegans ABC transporter PGP-2 in the biogenesis of a lysosome-related fat storage organelle.* Mol Biol Cell, 2007. **18**(3): p. 995-1008.
96. Rabbitts, B.M., et al., *glo-3, a novel Caenorhabditis elegans gene, is required for lysosome-related organelle biogenesis.* Genetics, 2008. **180**(2): p. 857-71.
97. Jo, H., et al., *IRE-1 and HSP-4 contribute to energy homeostasis via fasting-induced lipases in C. elegans.* Cell Metab, 2009. **9**(5): p. 440-8.
98. O'Rourke, E.J., et al., *C. elegans major fats are stored in vesicles distinct from lysosome-related organelles.* Cell Metab, 2009. **10**(5): p. 430-5.
99. Morck, C., et al., *Statins inhibit protein lipidation and induce the unfolded protein response in the non-sterol producing nematode Caenorhabditis elegans.* Proc Natl Acad Sci U S A, 2009. **106**(43): p. 18285-90.
100. Brooks, K.K., B. Liang, and J.L. Watts, *The influence of bacterial diet on fat storage in C. elegans.* PLoS One, 2009. **4**(10): p. e7545.
101. Soukas, A.A., et al., *Rictor/TORC2 regulates fat metabolism, feeding, growth, and life span in Caenorhabditis elegans.* Genes Dev, 2009. **23**(4): p. 496-511.
102. Hastie, C.J., H.J. McLauchlan, and P. Cohen, *Assay of protein kinases using*

radiolabeled ATP: a protocol. Nat Protoc, 2006. **1**(2): p. 968-71.

103. Dennis, G., Jr., et al., *DAVID: Database for Annotation, Visualization, and Integrated Discovery.* Genome Biol, 2003. **4**(5): p. P3.
104. Suzuki, R. and H. Shimodaira, *Pvclust: an R package for assessing the uncertainty in hierarchical clustering.* Bioinformatics, 2006. **22**(12): p. 1540-2.
105. Zhang, S.O., et al., *Genetic and dietary regulation of lipid droplet expansion in Caenorhabditis elegans.* Proc Natl Acad Sci U S A, 2010. **107**(10): p. 4640-5.
106. Zhang, P., et al., *Proteomic study and marker protein identification of Caenorhabditis elegans lipid droplets.* Mol Cell Proteomics, 2012. **11**(8): p. 317-28.
107. Lefevre, C., et al., *Mutations in CGI-58, the gene encoding a new protein of the esterase/lipase/thioesterase subfamily, in Chanarin-Dorfman syndrome.* Am J Hum Genet, 2001. **69**(5): p. 1002-12.
108. Hardie, D.G., F.A. Ross, and S.A. Hawley, *AMPK: a nutrient and energy sensor that maintains energy homeostasis.* Nat Rev Mol Cell Biol, 2012. **13**(4): p. 251-62.
109. Lee, H., et al., *The Caenorhabditis elegans AMP-activated protein kinase AAK-2 is phosphorylated by LKB1 and is required for resistance to oxidative stress and for normal motility and foraging behavior.* J Biol Chem, 2008. **283**(22): p. 14988-93.
110. Schade, M.A., et al., *Mutations that rescue the paralysis of Caenorhabditis elegans ric-8 (synembryn) mutants activate the G alpha(s) pathway and define a third major branch of the synaptic signaling network*. Genetics, 2005. **169**(2): p. 631-49.
111. Lu, X.Y., et al., *Cloning, structure, and expression of the gene for a novel regulatory subunit of cAMP-dependent protein kinase in Caenorhabditis elegans.* J Biol Chem, 1990. **265**(6): p. 3293-303.
112. Elle, I.C., et al., *Something worth dyeing for: molecular tools for the dissection of lipid metabolism in Caenorhabditis elegans.* FEBS Lett, 2010. **584**(11): p. 2183-93.
113. Large, V., et al., *Decreased expression and function of adipocyte hormone-sensitive lipase in subcutaneous fat cells of obese subjects.* J Lipid Res, 1999. **40**(11): p. 2059-66.
114. Reynisdottir, S., et al., *Effects of weight reduction on the regulation of lipolysis in adipocytes of women with upper-body obesity.* Clin Sci (Lond), 1995. **89**(4): p. 421-9.
115. Radner, F.P., et al., *Growth retardation, impaired triacylglycerol catabolism, hepatic steatosis, and lethal skin barrier defect in mice lacking comparative gene identification-58 (CGI-58).* J Biol Chem, 2010. **285**(10): p. 7300-11.
116. Xu, N., et al., *The FATP1-DGAT2 complex facilitates lipid droplet expansion at the ER-lipid droplet interface.* J Cell Biol, 2012. **198**(5): p. 895-911.
117. Martinez-Botas, J., et al., *Absence of perilipin results in leanness and reverses obesity*

in Lepr(db/db) mice. Nat Genet, 2000. **26**(4): p. 474-9.

118. Kurat, C.F., et al., *Cdk1/Cdc28-dependent activation of the major triacylglycerol lipase Tgl4 in yeast links lipolysis to cell-cycle progression.* Mol Cell, 2009. **33**(1): p. 53-63.
119. Gronke, S., et al., *Brummer lipase is an evolutionary conserved fat storage regulator in Drosophila.* Cell Metab, 2005. **1**(5): p. 323-30.
120. Lake, A.C., et al., *Expression, regulation, and triglyceride hydrolase activity of Adiponutrin family members.* J Lipid Res, 2005. **46**(11): p. 2477-87.
121. Miyoshi, H., et al., *Control of adipose triglyceride lipase action by serine 517 of perilipin A globally regulates protein kinase A-stimulated lipolysis in adipocytes.* J Biol Chem, 2007. **282**(2): p. 996-1002.
122. Dai, Z., et al., *Dual regulation of adipose triglyceride lipase by pigment epithelium-derived factor: a novel mechanistic insight into progressive obesity.* Mol Cell Endocrinol, 2013. **377**(1-2): p. 123-34.
123. Olzmann, J.A., C.M. Richter, and R.R. Kopito, *Spatial regulation of UBXD8 and p97/VCP controls ATGL-mediated lipid droplet turnover.* Proc Natl Acad Sci U S A, 2013. **110**(4): p. 1345-50.
124. Noble, T., J. Stieglitz, and S. Srinivasan, *An Integrated Serotonin and Octopamine Neuronal Circuit Directs the Release of an Endocrine Signal to Control C. elegans Body Fat.* Cell Metab, 2013.
125. Tan, K.T., et al., *Insulin/IGF-1 receptor signaling enhances biosynthetic activity and fat mobilization in the initial phase of starvation in adult male C. elegans.* Cell Metab, 2011. **14**(3): p. 390-402.
126. Gauthier, M.S., et al., *AMP-activated protein kinase is activated as a consequence of lipolysis in the adipocyte: potential mechanism and physiological relevance.* J Biol Chem, 2008. **283**(24): p. 16514-24.
127. Djouder, N., et al., *PKA phosphorylates and inactivates AMPKalpha to promote efficient lipolysis.* EMBO J, 2010. **29**(2): p. 469-81.
128. Czyzyk, T.A., et al., *Disruption of the RIIbeta subunit of PKA reverses the obesity syndrome of Agouti lethal yellow mice.* Proc Natl Acad Sci U S A, 2008. **105**(1): p. 276-81.
129. Mantovani, G., et al., *Protein kinase A regulatory subunits in human adipose tissue: decreased R2B expression and activity in adipocytes from obese subjects.* Diabetes, 2009. **58**(3): p. 620-6.
130. Jocken, J.W., et al., *Adipose triglyceride lipase and hormone-sensitive lipase protein expression is decreased in the obese insulin-resistant state.* J Clin Endocrinol Metab, 2007. **92**(6): p. 2292-9.

131. Steinberg, G.R., B.E. Kemp, and M.J. Watt, *Adipocyte triglyceride lipase expression in human obesity.* Am J Physiol Endocrinol Metab, 2007. **293**(4): p. E958-64.
132. Ryden, M., et al., *Comparative studies of the role of hormone-sensitive lipase and adipose triglyceride lipase in human fat cell lipolysis.* Am J Physiol Endocrinol Metab, 2007. **292**(6): p. E1847-55.
133. Fiorenza, C.G., S.H. Chou, and C.S. Mantzoros, *Lipodystrophy: pathophysiology and advances in treatment.* Nat Rev Endocrinol, 2011. **7**(3): p. 137-50.
134. Huang-Doran, I., et al., *Lipodystrophy: metabolic insights from a rare disorder.* J Endocrinol, 2010. **207**(3): p. 245-55.
135. Agustsson, T., et al., *Mechanism of increased lipolysis in cancer cachexia.* Cancer Res, 2007. **67**(11): p. 5531-7.
136. Das, S.K., et al., *Adipose triglyceride lipase contributes to cancer-associated cachexia.* Science, 2011. **333**(6039): p. 233-8.
137. Fearon, K.C., D.J. Glass, and D.C. Guttridge, *Cancer cachexia: mediators, signaling, and metabolic pathways.* Cell Metab, 2012. **16**(2): p. 153-66.

국문초록

지방의 분해는 다양한 세포 내 신호전달과 효소의 작용을 통해 조절되는 정교한 과정이다. PKA 신호전달경로는 지방대사물의 분해를 조절하는 주된 요인으로 알려져 있다. 하지만 현재까지 포유류 모델에서 PKA의 지방조절에 관한 연구는 PKA를 구성하는 단백질의 복잡함과 보상작용으로 인하여 제한점이 많다. 이러한 한계점을 극복하기 위하여, 본 연구에서는 *Caenorhabditis elegans*와 지방세포주 모델을 이용하여 PKA 의존적 지방대사물 분해에 연관된 유전자와 관련 메커니즘을 연구하였다. *C. elegans*와 지방세포주 모델은 RNAi를 이용한 유전자 억제를 통하여 PKA 활성을 효과적으로 조절할 수 있다는 장점이 있다.

*C. elegans*는 단식에 반응하여 저장된 지방대사물을 사용한다. 흥미롭게도, *C. elegans*에는 지방대사에 중요한 역할을 수행하는 perilipin 이라는 지방소체 단백질이 결여되어 있는데, 어떤 유전자가 이를 대체하여 지방분해과정을 매개하는지에 대해서는 알려져 있지 않다. 본 연구에서는 단식 상황이 *C. elegans*의 장세포 내 cAMP 농도 증가와 PKA 활성을 유도하고, PKA가 ATGL-1 지방분해효소와 LID-1이란 지방소체 단백질을 통하여 지방분해를 유도함을 증명하였다. LID-1 단백질은 ATGL-1과 결합하여 ATGL-1을 지방소체로 이동시키는 기능을 한다. ATGL-1이 결핍된 경우에는 저장된 지방대사물을 사용하지 못하며 ATGL-1을 과발현시킨 경우에는 지방대사물의 축적이 감소하였는데, 이 과정에 LID-1이 필요하다는 결과를 얻었다. ATGL-1 단백질은 PKA에 의해 인산화되고, 그로 인하여 단백질 안정성과 LID-1과의 결합이 증가하였다. 또한, *C. elegans* 야생형을 대상으로 EMS에 의한 무작위 돌연변이 스크리닝을 수행하여 PKA 기능을 억제할 수

있는 세 종류의 돌연변이 개체를 동정하였다. 이들 돌연변이는 *kin-2* RNAi에 의한 형태적인 변화와 Nile Red로 염색되는 granule의 감소 현상을 억제하였다. 이들 돌연변이 개체의 원인 유전자가 어떤 것인지는 추가적인 연구를 통하여 알아볼 것이다.

포유류 지방세포를 이용한 연구에서는, siRNA의 세포내 도입을 통하여 PKA의 RIα와 RIIβ 구성인자가 지방대사물 분해 조절에 필수적이라는 사실을 밝혀내었다. 또한, PKA의 RIα, RIIβ 구성인자의 억제를 통하여 PKA의 활성을 증가시킬 경우 ATGL 지방분해효소의 양적 증가가 관찰되었으며, 이는 ATGL이 PKA 의존적 지방대사물 분해과정에 주된 역할을 한다는 결과와 일치한다. 그리고 고지방식이를 통하여 비만을 유도한 생쥐 모델의 경우 지방조직에서 PKA RIIβ 구성인자의 발현이 감소하는 것을 관찰할 수 있었고, 이러한 현상은 비만 개체의 고지혈증과 PKA 발현이 연계되어 있을 가능성을 제시한다. 종합적으로 본 연구의 결과들은 지방대사의 항상성 조절에 있어서 PKA에 의한 지방분해효소와 지방소체 단백질의 조절이 중요함을 제시한다.

주요어 : PKA, 지방분해, ATGL, 지방소체

학번 : 2007 – 20359